Nonclassical vs Classical Metal···H₃C−C Interactions: Accurate Characterization of a 14-Electron Ruthenium(II) System by Neutron Diffraction, Database Analysis, Solution Dynamics, and DFT Studies

Walter Baratta,*,† Carlo Mealli,*,‡ Eberhardt Herdtweck,§ Andrea Ienco,‡
Sax A. Mason,‖ and Pierluigi Rigo†

*Contribution from Dipartimento di Scienze e Tecnologie Chimiche, Università di Udine,
Via Cotonificio 108, I-33100 Udine, Italy, Istituto di Chimica dei Composti Organometallici
(ICCOM-CNR), Via Madonna del Piano, I-50019 Sesto Fiorentino (Firenze), Italy,
Anorganisch-chemisches Institut, Technische Universität München, Lichtenbergstrasse 4,
D-85747 Garching, Germany, and Institut Max von Laue−Paul Langevin, 6,
Rue Jules Horowitz, BP 156, F-38042 Grenoble Cedex 9, France*

Received October 10, 2003; E-mail: inorg@dstc.uniud.it; mealli@iccom.cnr.it

Abstract: A neutron diffraction study of the complex RuCl₂[PPh₂(2,6-Me₂C₆H₃)]₂ (**1**) defines the precise nature of the δ agostic interactions between the unsaturated metal center and two *o*-methyl groups of the xylyl substituents. The CH₃ carbon atoms lie in the RuP₂ equatorial plane with Ru···C distances of 2.637(7) and 2.668(6) Å, whereas four short Ru···H distances (from 2.113(11) to 2.507(11) Å) indicate that each methyl group interacts with two C−H bonds. A survey of the X-ray structures with β, γ, δ, and ϵ M···H₃C−C moieties (no neutron data have been previously reported) shows a linear correlation between the angle M···C−C and the torsion of the methyl group about the C−C bond. Thus, the agostic interactions span the range between the classical (M···η^2-HC) and the nonclassical (M···η^3-H₂C) types. A solution study of **1** shows intramolecular rearrangement of each xylyl substituent that equilibrates the environments of its two *ortho* CH₃ groups. Activation parameters, evaluated from the analysis of ¹H NMR line shape as a function of temperature, are $\Delta H^{\ddagger} = 9.6 \pm 0.2$ kcal mol⁻¹ with $\Delta S^{\ddagger} = -15.4 \pm 0.7$ eu (CDCl₃). The related 14-electron complexes RuX₂[PPh₂(2,6-Me₂C₆H₃)]₂ (X = I, **2**; NCO, **3**), prepared from **1** and NaX, show a similar dynamic process in solution, with the iodo derivative displaying the most hindered rotation of the xylyl group. A DFT optimization of the complex RuCl₂[PH₂(2,6-Me₂C₆H₃)]₂ (**1a**) reproduces well the nonclassical Ru···η^3-H₂C agostic mode, whereas the classical Ru···η^2-HC one corresponds to a transition state **1b**, destabilized by 3.4 kcal mol⁻¹. A similar barrier (ca. 3.8 kcal mol⁻¹) is calculated for the xylyl rotation in the further simplified model RuCl₂[PH₂(2,6-Me₂C₆H₃)][PH₂CH=CHCH₃] (**1c**), the absence of bulky phenyl substituents being largely responsible for the difference with respect to the experimental value. Finally, the MO analysis addresses the intrinsic stability of the 14-electron complex RuCl₂(PH₃)₂ and, in agostic complexes, accounts for the different interactions between the methyl group and the metal atom in relation to the length of their interconnecting chain.

Introduction

The coordination of inert C−H bonds to a transition metal is of fundamental interest for stoichiometric and catalytic reactions, with particular regard to the problem of alkane functionalization via C−H bond activation.[1] Great attention has been devoted to the fate of an alkane molecule that approaches an unsaturated metal fragment or metal surface. Unfortunately, information on the nature of the primary adduct is still very scarce, since

saturated hydrocarbons are notoriously unreactive and are very poor ligands.[1d] To the best of our knowledge, the adduct between an iron(II) porphyrin complex and an *n*-heptane molecule is the only confirmed example of such an intermolecular interaction, although its structural characterization is rather poor,[2a] whereas other examples of alkane complexes have been reported in matrix-isolated, solution and gas phases.[1d,2b] From the DFT calculations on simpler adducts between an unsaturated metal center and a methane molecule, a somewhat asymmetric M···η^3-H₂C bonding mode has emerged.[3] In general, the metal lies in one CH₂ plane of the alkane with two short but distinct M···H distances. This result is in apparent disagreement with

---

† Università di Udine.
‡ Istituto di Chimica dei Composti Organometallici.
§ Technische Universität München.
‖ Institut Max von Laue−Paul Langevin.

(1) (a) Labinger, J. A.; Bercaw, J. E. *Nature* **2002**, *417*, 507. (b) Crabtree, R. H. *J. Chem. Soc., Dalton Trans.* **2001**, 2437. (c) Shilov, A. E.; Shul'pin, G. B. *Chem. Rev.* **1997**, *97*, 2879. (d) Hall, C.; Perutz, R. N. *Chem. Rev.* **1996**, *96*, 3125. (e) Ryabov, A. D. *Chem. Rev.* **1990**, *90*, 403.

(2) (a) Evans, D. R.; Drovetskaya, T.; Bau, R.; Reed, C. A.; Boyd, P. D. W. *J. Am. Chem. Soc.* **1997**, *119*, 3633. (b) Geftakis, S.; Ball, G. E. *J. Am. Chem. Soc.* **1998**, *120*, 9953.

---

the rich experimental and theoretical information available for agostic complexes that are generally interpreted in terms of *dihapto M···η^2-HC* bonding between the unsaturated metal ion and a dangling C−H bond of the same molecular fragment.[4]

Bulky phosphines of the type PR$_3$ (R = Ph, ^{i}Pr, Cy) have been successfully used for the preparation of coordinatively unsaturated metal complexes that are stabilized by γ agostic interactions.[4a−c] The hydrocarbon moiety at one arm of the ligand may donate electrons to the empty orbitals of the metal, preventing solvent coordination or dimerization of the complex. In general, the length of the arm that connects the metal and a dangling CH group (β through ϵ connectivity) seems to be an important factor for the strength of the agostic interactions. This point is stressed in the present article, which analyzes experimental and computational aspects of the recently reported 14-electron ruthenium(II) complex RuCl$_2$[PPh$_2$(2,6-Me$_2$C$_6$H$_3$)]$_2$ (**1**).[5] As inferred also from the 14-electron T-shaped platinum-(II) species [Pt(P-C){PR$_2$(2,6-Me$_2$C$_6$H$_3$)}]$^+$ (P-C = PR$_2$(2-CH$_2$-6-MeC$_6$H$_3$); R = Ph, Cy),[6] unique bonding features are attributable to the new class of ligands PR$_2$(2,6-Me$_2$C$_6$H$_3$). The phenyl or the cyclohexyl substituents could in principle stabilize a γ agostic interaction, but the involvement of the xylyl substituent gives rise to a δ agostic interaction with the formation of a "five-membered" ring closed by the carbon of the *o*-methyl group.

As regards ruthenium(II) coordination chemistry, phosphines with a small cone angle give 18-electron octahedral complexes of the type RuX$_2$(PR$_3$)$_4$ (X = halide).[7] Bulkier arylphosphines form five-coordinate 16-electron species [e.g., RuCl$_2$(PPh$_3$)$_3$] that are stabilized by the γ agostic interaction of the *ortho* C−H bond.[8] Finally, there are few examples of 14-electron ruthenium(II) complexes, such as Ru(SC$_6$F$_5$)$_2$(PPh$_3$)$_2$,[9] Ru(O^{t}Bu)$_2$-(=CHPh)(PCy$_3$),[10] the imidazole derivative RuCl$_2$(L)$_2$,[11] and the recently reported paramagnetic complex RuCl(PNP^{tBu}).[12] Conversely, the comparable species Ru(OC$_6$Cl$_5$)$_2$(PPh$_2$CH$_2$-CH$_2$P^{i}Pr$_2$)[13] is best considered as an 18-electron complex, since
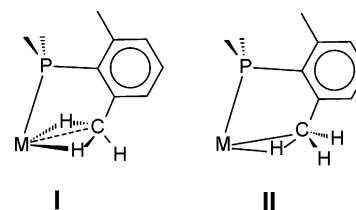
Figure 1. Types of M···H$_3$C agostic interactions (M···η^3-H$_2$C vs classical M···η^2-HC).

the two *o*-chlorine donor atoms complete the octahedral geometry. Incidentally, the complex RuHCl(P^{i}Pr$_3$)$_2$, which was originally described by Caulton and subsequently by van der Schaaf as a 14-electron species,[14] was finally reported by Caulton[15] and recorrected by van der Schaff[14b] as a binuclear complex with Ru(μ-Cl)Ru bridges, as in the complexes of stoichiometry [RuCl$_2$(PR$_3$)$_2$]$_2$ (R = Ph, 3-C$_6$H$_4$SO$_3$H).[16] In this regard, it is noteworthy that the related 16-electron dihydrogen complexes RuXX′(H$_2$)L$_2$ (X, X′ = halogen, H; L = P^{i}Pr$_3$, P^{t}Bu$_2$Me) have been used as suitable precursors of 14-electron species RuXX′L$_2$ for the preparation of ruthenium(II) carbene and vinylidene derivatives.[17]

The stabilization of **1** is attributable to the exceptional steric requirements of the ligand PPh$_2$(2,6-Me$_2$C$_6$H$_3$), which features two *o*-methyl groups. Interestingly, by reaction of osmium derivatives with this phosphine, we have obtained complexes that contain a tridentate *trans*-stilbene-type ligand, as a result of the coupling between two *o*-methyl groups via the activation of four C−H bonds.[18]

The already reported X-ray analyses of **1** and the related T-shaped platinum(II) complex [Pt(P-C){PCy$_2$(2,6-Me$_2$C$_6$H$_3$)}]$^+$ highlighted some unusual aspects. Thus, the skeleton of uncharged species **1**,[5] unlike those of other 14-electron analogues, such as the cations [RuPh(CO)(P^{t}Bu$_2$Me)$_2$]$^+$ [19] or [Ir(H)$_2$-(P^{t}Bu$_2$Ph)$_2$]$^+$,[20] features two *cis* rather than *trans* phosphine ligands. Moreover, the δ methyl agostic interactions appear peculiar. As sketched in Figure 1, the observed stereochemistry for **1** seems much closer to type **I** (with a η^3 coordinated CH$_2$ group) than to the more classical M···η^2-HC coordination mode **II**. The type **I** is further supported by the T-shaped platinum-(II) complex that features two almost equivalent M···H distances.[6]

To establish the apparently unusual stereochemistry of **1**, suitable crystals were prepared for a neutron diffraction study,

(3) (a) Hill, G. S.; Puddephatt, R. J. *Organometallics* **1998**, *17*, 1478. (b) Song, J.; Hall, M. B. *Organometallics* **1993**, *12*, 3118. (c) Koga, N.; Morokuma, K. *J. Am. Chem. Soc.* **1993**, *115*, 6883. (d) Margl, P.; Ziegler, T.; Blöchl, P. E. *J. Am. Chem. Soc.* **1995**, *117*, 12625. (e) Heiberg, H.; Hohansson, L.; Gropen, O.; Ryan, O. B.; Swang, O.; Tilset, M. *J. Am. Chem. Soc.* **2000**, *122*, 10831. (f) Janak, K. E.; Churchill, D. G.; Parkin, G. *Chem. Commun.* **2003**, 22. (g) Green, J. C.; Harvey, J. N.; Poli, R. *J. Chem. Soc., Dalton Trans.* **2002**, 1861.
(4) (a) Brookhart, M.; Green, M. L. H.; Wong, L.-L. *Prog. Inorg. Chem.* **1988**, *36*, 1. (b) Crabtree, R. H.; Hamilton, D. G. *Adv. Organomet. Chem.* **1988**, *28*, 299. (c) Crabtree, R. H. *Angew. Chem., Int. Ed. Engl.* **1993**, *32*, 789. (d) Yao, W.; Eisenstein, O.; Crabtree, R. H. *Inorg. Chim. Acta* **1997**, *254*, 105. (e) Ogasawara, M.; Saburi, M. *Organometallics* **1994**, *13*, 1911.
(5) Baratta, W.; Herdtweck, E.; Rigo, P. *Angew. Chem., Int. Ed.* **1999**, *38*, 1629.
(6) Baratta, W.; Stoccoro, S.; Doppiu, A.; Herdtweck, E.; Zucca, A.; Rigo, P. *Angew. Chem., Int. Ed.* **2003**, *42*, 105.
(7) (a) Schröder, M.; Stephenson, T. A. In *Comprehensive Coordination Chemistry*; Wilkinson, G., Gillard, R. D., McCleverty, J. A., Eds.; Pergamon Press: Oxford, 1987; Vol. 4, p 377 and references therein. (b) Seddon, E. A.; Seddon, K. R. In *The Chemistry of Ruthenium*; Clark, R. J. H., Ed.; Elsevier: Amsterdam, 1984; p 487. (c) Jardine, F. H. *Prog. Inorg. Chem.* **1984**, *31*, 265.
(8) (a) Stephenson, T. A.; Wilkinson, G. *J. Inorg. Nucl. Chem.* **1966**, *28*, 945. (b) La Placa, S. J.; Ibers, J. A. *Inorg. Chem.* **1965**, *4*, 778.
(9) (a) Catalá, R.-M.; Cruz-Garritz, D.; Terreros, P.; Torrens, H.; Hills, A.; Hughes, D. L.; Richards, R. L. *J. Organomet. Chem.* **1987**, *328*, C37. (b) Catalá, R.-M.; Cruz-Garritz, D.; Sosa, P.; Terreros, P.; Torrens, H.; Hills, A.; Hughes, D. L.; Richards, R. L. *J. Organomet. Chem.* **1989**, *359*, 219.
(10) Sandford, M. S.; Henling, L. M.; Day, M. W.; Grubbs, R. H. *Angew. Chem., Int. Ed.* **2000**, *39*, 3451.
(11) Sánchez-Delgado, R. A.; Navarro, M.; Lazardi, K.; Atencio, R.; Capparelli, M.; Vargas, F.; Urbina, J. A.; Bouillez, A.; Noels, A. F.; Masi, D. *Inorg. Chim. Acta* **1998**, *275−276*, 528.
(12) Watson, L. A.; Ozerov, O. V.; Pink, M.; Caulton, K. G. *J. Am. Chem. Soc.* **2003**, *125*, 8426.

(13) Fries, G.; Wolf, J.; Pfeiffer, M.; Stalke, D.; Werner, H. *Angew. Chem., Int. Ed.* **2000**, *39*, 564.
(14) (a) Coalter, J. N.; Spivak, G. J.; Gérard, H.; Clot, E.; Davidson, E. R.; Eisenstein, O.; Caulton, K. G. *J. Am. Chem. Soc.* **1998**, *120*, 9388. (b) van der Schaaf, P. A.; Kolly, R.; Hafner, A. *Chem. Commun.* **2000**, 1045; see also corrigendum: *Chem. Commun.* **2001**, 940.
(15) (a) Coalter, J. N.; Huffman, J. C.; Streib, W. E.; Caulton, K. G. *Inorg. Chem.* **2000**, *39*, 3757. (b) Coalter, J. N.; Streib, W. E.; Caulton, K. G. *Inorg. Chem.* **2000**, *39*, 3749. (c) Coalter, J. N.; Huffman, J. C.; Caulton, K. G. *Organometallics* **2000**, *19*, 3569.
(16) (a) Hoffmann, P. R.; Caulton, K. G. *J. Am. Chem. Soc.* **1975**, *97*, 4221. (b) Armit, P. W.; Boyd, A. S. F.; Stephenson, T. A. *J. Chem. Soc., Dalton Trans.* **1975**, 1663. (c) Tóth, Z.; Joó, F.; Beck, M. T. *Inorg. Chim. Acta* **1980**, *42*, 153. (d) Joó, F.; Kovács, J.; Kathó, A.; Bényei, A. C.; Decuir, T.; Darensbourg, D. J. *Inorg. Synth.* **1998**, *32*, 1.
(17) (a) Wolf, J.; Stüer, W.; Grünwald, C.; Werner, H.; Schwab, P.; Schulz, M. *Angew. Chem., Int. Ed.* **1998**, *37*, 1124. (b) Oliván, M.; Clot, E.; Eisenstein, O.; Caulton, K. G. *Organometallics* **1998**, *17*, 3091.
(18) Baratta, W.; Herdtweck, E.; Martinuzzi, P.; Rigo, P. *Organometallics* **2001**, *20*, 305.
(19) Huang, D.; Streib, W. E.; Eisenstein, O.; Caulton, K. G. *Angew. Chem., Int. Ed. Engl.* **1997**, *36*, 2004.
(20) Cooper, A. C.; Streib, W. E.; Eisenstein, O.; Caulton, K. G. *J. Am. Chem. Soc.* **1997**, *119*, 9069.
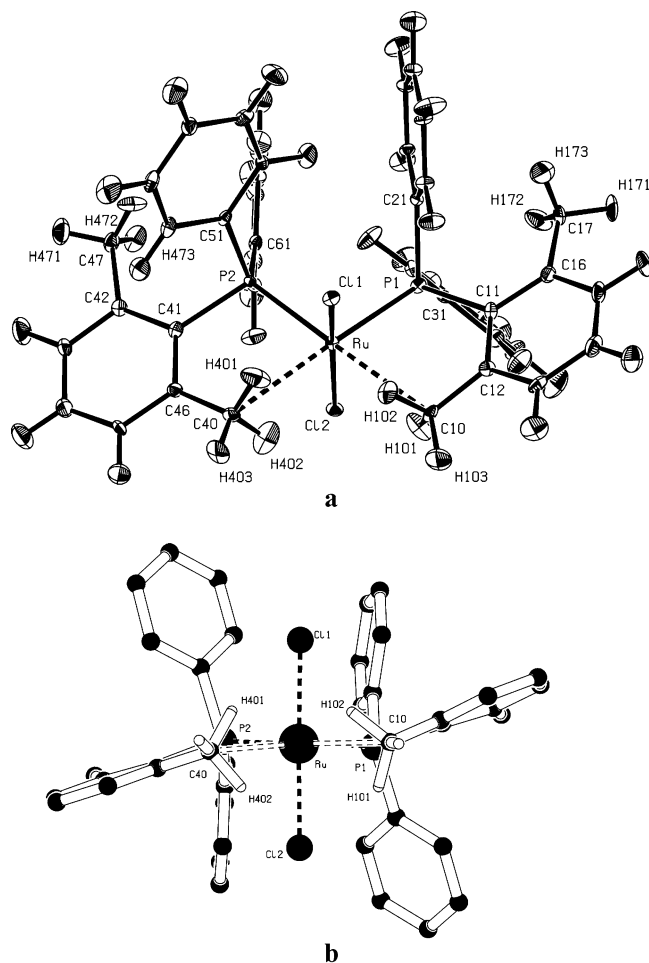
Figure 2. (a) ORTEP representation of complex **1** in the solid state. Thermal ellipsoids are at the 30% probability level. (b) Drawing down the pseudo C_2 axis (hydrogen atoms are omitted except for those of agostic CH$_3$ groups).

a technique that has rarely been adopted to establish the precise nature of agostic interactions.[21] Furthermore, we carried out accurate NMR studies in solution to assess chemical shifts and energetic parameters associated with the fluxionality of the xylyl groups. This study has also been extended to the other two congeners RuX$_2$[PPh$_2$(2,6-Me$_2$C$_6$H$_3$)]$_2$ (X = I, **2**; NCO, **3**)].

In view of the experimental results, we have systematically examined all the available structures of the Cambridge Structural Database[22a] that feature either an intra- or an intermolecular M•••H$_3$C interaction. This study has confirmed that the agostic interactions actually fall between the two limits **I** and **II**, and it has clarified the basic geometric parameters governing the trends. These points have been further substantiated by DFT and MO studies carried out for model complexes of **1** as well as for the adduct between the simplest 14-electron species RuCl$_2$-(PH$_3$)$_2$ and two methane molecules.

Results and Discussion

Neutron Diffraction Study of 1. An ORTEP drawing of compound **1**, as obtained from the neutron diffraction measurements performed at 100 K, is shown in Figure 2a. Ordered solvent toluene molecules are also found in the crystal lattice. The complex has almost C_2 symmetry, and its ML$_4$ skeleton, with a butterfly shape, may be thought of as derived from an octahedron upon the removal of two *cis* equatorial

ligands. Coordinatively unsaturated 14-electron species of this type are therefore characterized by two empty σ hybrid orbitals in the direction of the missing ligands (one σ plus one d$_\pi$ orbital, in MO terms). Disregarding for the moment any Ru•••H interaction, two methyl carbon atoms (C10 and C40) are close to the fifth and sixth positions of the octahedron with rather short Ru•••C distances (2.668(6) and 2.637(7) Å). The deviation of these carbon atoms from the Ru,P1,P2 plane is small (Δ = 0.078(3) Å), whereas the angles P2−Ru−C10 and P1−Ru−C40 are linear within 5°. The *cis* arrangement of the two phosphine ligands is remarkable, in comparison with the *trans* arrangement found in other butterfly 14-electron cations [RuPh(CO)(P^{t}Bu$_2$Me)$_2$]$^+$ [19] or [Ir(H)$_2$(P^{t}Bu$_2$Ph)$_2$]$^+$ [20] and may be attributed to the π donor effects of the chloride ligands, as will be shown below from MO considerations.

As shown in Table 1, there is good agreement between the geometric parameters from the neutron and the X-ray measurements,[5] at least for the non-hydrogen backbone atoms. The *trans* axial Cl−Ru−Cl angle is somewhat closed [167.7(2)°] with the two Cl atoms moving away from the phosphine donors. This situation was also observed in the related Ru(II) complexes RuCl$_2$(PPh$_2$Ar)$_2$ (Ar = 2-MeOC$_6$H$_4$, 2,6-(MeO)$_2$C$_6$H$_3$), which are octahedral with the *cis* positions occupied by the oxygen donors belonging to the phosphine aryl substituents.[23] In **1**, the Ru−P−C$_{ipso}$ angles are significantly more closed for the xylyl (109.2(3)° and 110.0(3)°) than for the phenyl substituents (115.0(3)−118.7(3)°). These geometric details are clearly indicative of the forces exerted by the δ-agostic Ru•••H$_3$C interactions. An even larger effect is observed in γ-agostic analogues, such as the cation [Ru(CO)(P^{t}Bu$_2$Me)$_2$(η^2-Me$_3$SiCH= CHC=CHSiMe$_3$)]$^+$,[24] in which the Ru−P−C$_{ipso}$ angle involved in the agostic interaction is as small as ca. 99°, whereas the remaining two Ru−P−C$_{ipso}$ angles are definitely more open.

Although in **1** two methyl carbon atoms are essentially in the Ru,P1,P2 plane, the dihedral angles formed by the latter plane and the two xylyl substituents are about 20°. The rotations of the latter about their pivotal linkages P1−C11 and P2−C41 help to release the steric hindrance between the facing phenyl substituents of the two phosphine ligands. Such a viewpoint is supported by the structure of the complex [Pt(P-C){PCy$_2$(2,6-Me$_2$C$_6$H$_3$)}]$^+$,[6] in which the phosphorus atoms are *trans* and the xylyl group is coplanar. Interestingly, no additional rearrangement of the ligand PPh$_2$(2,6-Me$_2$C$_6$H$_3$) seems necessary to achieve the metal coordination in **1**. Thus, for the two phosphines the dihedral angle formed by the plane of the three C$_{ipso}$ atoms and the xylyl group is almost identical [75.1(1)° and 76.1(1)°] to that of the free phosphine PPh$_2$(2,4,6-Me$_3$C$_6$H$_2$) (76.9(1)°),[25] and this is observed also for the dihedral angles involving the phenyl substituents.

(21) (a) Cole, J. M.; Gibson, V. C.; Howard, J. A. K.; McIntyre, G. J.; Walker, G. L. P. *Chem. Commun.* **1998**, 1829. (b) Bau, R.; Mason, S. A.; Patrick, B. O.; Adams, C. S.; Sharp, W. B.; Legzdins, P. *Organometallics* **2001**, *20*, 4492. (c) Klooster, W. T.; Brammer, L.; Schaverien, C. J.; Budzelaar, P. H. M. *J. Am. Chem. Soc.* **1999**, *121*, 1381. (d) Klooster, W. T.; Lu, R. S.; Anwander, R.; Evans, W. J.; Koetzle, T. F.; Bau, R. *Angew. Chem., Int. Ed.* **1998**, *37*, 1268.
(22) (a) Allen, F. H.; Kennard, O. *Chem. Des. Autom. News* **1993**, *8*, 31. (b) Braga, D.; Grepioni, F.; Biradha, K.; Desiraju, G. R. *J. Chem. Soc., Dalton Trans.* **1996**, 3925. (c) Brammer, L. *Dalton Trans.* **2003**, 3145.
(23) (a) Yamamoto, Y.; Sato, R.; Matsuo, F.; Sudoh, C.; Igoshi, T. *Inorg. Chem.* **1996**, *35*, 2329. (b) Jeffrey, J. C.; Rauchfuss, T. B. *Inorg. Chem.* **1979**, *18*, 2658.
(24) Huang, D.; Olivan, M.; Huffman, J. C.; Eisenstein, O.; Caulton, K. G. *Organometallics* **1998**, *17*, 4700.

Table 1. Comparison of Selected Bond Distances (Å) and Angles (deg) Obtained from the Neutron and X-ray Diffraction Studies of RuCl$_2$[PPh$_2$(2,6-Me$_2$C$_6$H$_3$)]$_2$ (1·Toluene) and Selected Parameters Calculated for the Model Complex RuCl$_2$[PH$_2$(2,6-Me$_2$C$_6$H$_3$)]$_2$ (**1a**)

	1·toluene		
	neutron	X-ray[a]	**1a** DFT
Ru−Cl1	2.401(4)	2.3994(4)	2.45
Ru−Cl2	2.403(5)	2.3976(4)	2.45
Ru−P1	2.261(6)	2.2582(4)	2.23
Ru−P2	2.237(6)	2.2525(3)	2.23
Ru···C10	2.668(6)	2.6534(16)	2.79
Ru···C40	2.637(7)	2.6486(16)	2.79
Ru···H101	2.507(11)	2.33(2)	2.64
Ru···H102	2.113(11)	2.20(2)	2.18
Ru···H401	2.137(12)	2.19(2)	2.18
Ru···H402	2.399(14)	2.30(3)	2.64
Cl1···H102	2.407(10)	2.52(2)	
Cl1···H401	2.478(13)	2.66(2)	
Cl2···H101	2.576(11)	2.67(2)	
Cl2···H402	2.461(12)	2.56(3)	
C10−H101	1.083(13)	0.91(2)	
C10−H102	1.119(11)	0.96(2)	
C10−H103	1.093(13)	0.93(2)	
C17−H171	1.109(11)	0.96(3)	
C17−H172	1.065(14)	0.98(2)	
C17−H173	1.038(15)	0.97(2)	
C40−H401	1.111(14)	0.90(2)	
C40−H402	1.088(13)	0.93(3)	
C40−H403	1.084(12)	0.97(2)	
C47−H471	1.082(12)	1.00(2)	
C47−H472	1.099(12)	1.00(2)	
C47−H473	1.074(12)	0.99(2)	
Cl1−Ru−Cl2	167.7(2)	168.00(2)	176
Cl1−Ru−P1	95.2(2)	94.69(2)	
Cl1−Ru−P2	93.4(2)	92.93(2)	
Cl2−Ru−P1	91.6(2)	92.42(2)	
Cl2−Ru−P2	95.3(2)	95.05(2)	
P1−Ru−P2	101.6(2)	101.91(1)	97
C10···Ru···C40	102.4(2)	102.18(5)	
C10···Ru−P1	78.1(2)	78.17(4)	
C10···Ru−P2	177.7(2)	177.01(4)	
C40···Ru−P2	78.2(2)	77.94(4)	
C40···Ru−P1	174.8(2)	176.14(4)	
Ru−P1−C11	109.2(3)	109.21(5)	114
Ru−P1−C21	115.7(3)	116.40(4)	
Ru−P1−C31	117.7(3)	117.03(4)	
Ru−P2−C41	110.0(3)	109.53(4)	114
Ru−P2−C51	115.0(3)	115.74(4)	
Ru−P2−C61	118.7(3)	118.07(4)	
C12−C10···Ru	105.9(3)	106.54(9)	
C46−C40···Ru	107.7(3)	107.23(10)	
H101−C10−H102	112.0(8)	108(2)	
H101−C10−H103	104.2(10)	110(2)	
H102−C10−H103	104.0(9)	107(2)	
H401−C40−H402	110.4(10)	104(2)	
H401−C40−H403	103.8(10)	110(2)	
H402−C40−H403	104.8(10)	108(2)	

[a] X-ray values are from ref 5.

Importantly, the neutron diffraction study of **1** allows the correct and accurate location of the *o*-methyl hydrogen atoms, particularly of those interacting with the metal. It is confirmed that **1** features a double agostic arrangement of type **I** (Figure 1). Thus, two hydrogen atoms lie closer to the metal and are off the mean plane Ru,P1,P2,C10,C40 (Figure 2b). The third hydrogen atom is approximately in the latter plane, pointing away from the metal. The planes H101,C10,H102 and H401,C40,H402 are almost orthogonal to the Ru,P1,P2 equatorial plane (83(1)° and 75(1)°), whereas for each methyl group

(25) Blount, J. F.; Camp, D.; Hart, R. D.; Healy, P. C.; Skelton, B. W.; White, A. H. *Aust. J. Chem.* **1994**, *47*, 1631.

the two shorter Ru···H distances are clearly asymmetric (Ru···H101 = 2.507(11) Å, Ru···H102 = 2.113(10) Å and Ru···H401 = 2.137(12) Å, Ru···H402 = 2.399(14) Å). Although none of the latter values is as short as others reported for Ru···H agostic interactions of δ type (e.g., 1.89 Å is the average distance in [Ru$_2$(^{t}Bu$_2$PCH$_2$P^{t}Bu$_2$)$_2$(μ-Cl)$_3$]$^+$),[26] even the longest separation of 2.507(11) Å in **1** does not exclude a Ru···H interaction. Also, by overlooking the asymmetry of the two Ru···H distances, the ideal M···η^3-H$_2$C coordination is not achieved in this case since the metal is off the CH$_2$ plane, the dihedral angles Ru−H101−H102−C10 and Ru−H401−H402−C40 being about 150°. Also, on the basis of the available calculations for metal−methane adducts,[3] the M···η^3-H$_2$C coordination imposes an M···C−H$_{external}$ angle of about 125°, while in **1** the Ru···C−C angles are as small as 105.9(3)° and 107.7(3)°, respectively. Because the hydrogen atoms are more accurately located than from X-ray data, the elongation of the C−H distances closest to the metal is trustworthy in spite of nonnegligible standard deviations. Even more reliable are the differences between the angular values, in particular the evident opening of the H−C−H angles subtended by the metal atom. Thus, the values 112.0(8)° and 110.4(10)° of H101−C10−H102 and H401−C40−H402, respectively, are higher compared to the other H−C−H angles of the interacting (103.8(10)−104.8-(10)°) and noninteracting methyl groups (105.4(10)−108.1-(10)°). In conclusion, it is evident that the interaction with the metal affects significantly the geometry of the methyl group.

It is worth pointing out that ligands of the type PR$_2$(2,6-Me$_2$C$_6$H$_3$) (R = Ph, Cy) seem to favor strong agostic M···η^3-H$_2$C interactions. Also in the structure of the 14-electron Pt(II) cation,[6] in which the CH$_2$ plane almost bisects the ML$_3$ one, the Pt···C agostic distance (2.432(6) Å) is among the shortest for systems other than the α or the β type.

NMR Studies on 1. The variable temperature ^{31}P NMR spectra of **1** over the range −60 to +60 °C exhibit one sharp signal at about δ 56 (CDCl$_3$), close to that of the octahedral complex RuCl$_2${PPh$_2$[2,6-(MeO)$_2$C$_6$H$_3$]}$_2$ (δ 61.1),[23a] that contains a P,O hemilabile ligand.[27] This indicates that in **1** neither the rearrangement of the RuCl$_2$P$_2$ core nor the dissociation of the phosphine ligand occurs.

The room temperature ^{1}H NMR spectrum of **1** in CD$_2$Cl$_2$ shows two broad and equally intense peaks at δ 2.35 and 1.30 for the four methyl groups. At −50 °C the latter signal becomes sharp, whereas that at 2.35 appears as a doublet with a J_{HP} of 5.1 Hz. This resonance, attributable to the methyl groups close to ruthenium, slightly broadens at lower temperatures, but remains a single peak even at −120 °C (CD$_2$Cl$_2$/CFCl$_3$). This indicates that the rotation of the methyl groups about their C−CH$_3$ bonds cannot be frozen out.[28] The signal at δ 1.30 is consistent with the data of the related 18-electron ruthenium[29] and osmium[18] complexes bearing the *ortho* methyl phosphines PPh$_2$Ar (Ar = 2-MeC$_6$H$_4$, 2,6-Me$_2$C$_6$H$_3$), which show a reso-

(26) Hansen, S. M.; Rominger, F.; Metz, M.; Hofmann, P. *Chem. Eur. J.* **1999**, *5*, 557.

(27) (a) Lindner, E.; Geprägs, M.; Gierling, K.; Fawzi, R.; Steimann, M. *Inorg. Chem.* **1995**, *34*, 6106. (b) Lindner, E.; Möckel, A; Mayer, H. A.; Kühbauch, H.; Fawzi, R.; Steimann, M. *Inorg. Chem.* **1993**, *32*, 1266. (c) Lindner, E.; Karle, B. *Chem. Ber.* **1990**, *123*, 1469.
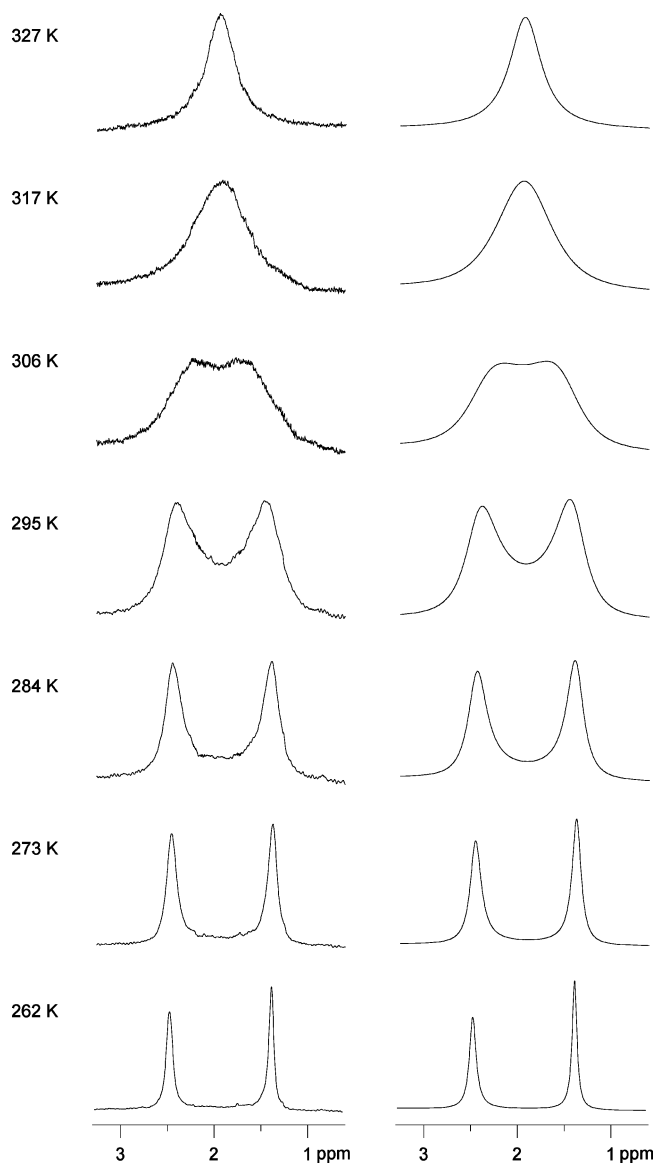
(28) The ^{1}H NMR spectrum of the free phosphine PPh$_2$(2,6-Me$_2$C$_6$H$_3$) exhibits one singlet at δ 2.20 for the *o*-methyl groups, and this signal remains sharp at −95 °C, indicating a free rotation of the xylyl group. In the ^{13}C NMR spectrum the signal for the methyls is a doublet at δ 23.4 with a $^3J_{CP}$ of 16.9 Hz.

nance of the methyls shifted upfield with respect to free ligand.[28] In **1** the resonance of the δ-agostic *ortho* methyl groups is slightly shifted downfield, and such a result clearly differs from the data of the "classical agostic" complexes, which generally exhibit proton signals at high field (δ_H < 0),[4a] except a few cases of Pt(II) and Pd(II) species that show a M···H−C interaction along the axial fifth position.[30] Although the high-field ^{1}H NMR chemical shift of agostic complexes is not clearly rationalized, for low-valent transition metal hydrides the negative values of δ_H have been ascribed to paramagnetic contributions from the adjacent metal fragment.[31]

At room temperature, the ^{13}C{^{1}H} NMR spectrum of **1** exhibits two broad signals for the methyl groups at δ 23.7 and 11.7. Upon cooling, the first resonance becomes sharp, whereas the second absorption, which is attributable to the interacting methyl groups, splits into a pseudo triplet with a $|^{trans}J_{CP} + {}^{cis}J_{CP}|$ of 23.6 Hz due to the $^2J_{PP}$ virtual coupling constant (−50 °C).[32] For complex **1**, the high-field signal is significantly affected by the temperature (11.7 at +20 °C, 10.1 at −40 °C, and 9.4 at −80 °C), in contrast with that at 23.7. In the ^{13}C NMR INEPT spectrum at − 40 °C, the latter signal is a sharp quartet with $^1J_{CH}$ = 127 Hz, whereas the resonance at δ 10.1 appears as a broad quartet with a lower value of $^1J_{CH}$ (117 Hz), which is consistent with the presence of an agostic interaction.[4a] Furthermore, a [1]H−^{13}C NMR experiment for **1** shows unambiguously that the high-field ^{13}C NMR signal for the agostic methyl group is correlated with the low-field ^{1}H NMR signal. Despite the paucity of ^{13}C NMR data for agostic complexes, an upfield shift has been reported for ruthenium(II)[26,33] and iridium(III)[34] derivatives. In the aromatic region, the ^{13}C{^{1}H} NMR spectrum shows two nonbinomial quintets at δ 134.5 and 132.0 in a 1:2 intensity ratio for the *ipso* carbon atoms of the xylyl and the phenyl groups, in agreement with the *cis* arrangement of the two phosphine ligands.[35]

The ^{1}H NMR spectra of **1** in CDCl₃ are temperature dependent, and Figure 3 shows the *o*-methyl group region between −11 and 54 °C.

At −11 °C the spectrum exhibits two resonances at δ 2.42 and 1.35 that on raising the temperature coalesce at 35 °C to a single averaged peak at δ 1.90, indicating a two site exchange process for the four methyl groups. The approximation to the Eyring equation $\Delta G^\ddagger = RT_c[22.96 + \ln(T_c/\Delta\nu)]$[36] ($\Delta\nu$ = 220 Hz) affords a $\Delta G^\ddagger_{308}$ = 14.3 ± 0.2 kcal/mol for the rotation of

(29) (a) Baratta, W.; Del Zotto, A.; Rigo, P. *Organometallics* **1999**, *18*, 5091. (b) Baratta, W.; Del Zotto, A.; Herdtweck, E.; Vuano, S.; Rigo, P. *J. Organomet. Chem.* **2001**, *617−618*, 511.
(30) (a) Albinati, A.; Pregosin, P. S.; Wombacher, F. *Inorg. Chem.* **1990**, *29*, 1812. (b) Roe, D. M.; Bailey, P. M.; Moseley, K.; Maitlis, P. *J. Chem. Soc., Chem. Commun.* **1972**, 1273. (c) van der Poel, H.; van Koten, G.; Vrieze, K. *Inorg. Chem.* **1980**, *19*, 1145. (d) Deeming, A. J.; Rothwell, I. P.; Hursthouse, M. B.; Malik, K. M. A. *J. Chem. Soc., Dalton Trans.* **1980**, 1974.
(31) Ruiz-Morales, Y.; Schreckenbach, G.; Ziegler, T. *Organometallics* **1996**, *15*, 3920.
(32) (a) Redfield, D. A.; Cary, L. W.; Nelson, J. H. *Inorg. Chem.* **1975**, *14*, 50. (b) Kemmitt, R. D. W.; McKenna, P.; Russell, D. R.; Sherry, L. J. S. *J. Chem. Soc., Dalton Trans.* **1985**, 259.
(33) (a) Perera, S. D.; Shaw, B. L. *J. Chem. Soc., Dalton Trans.* **1995**, 3861. (b) Takahashi, Y.; Hickichi, S.; Akita, M.; Moro-oka, Y. *Organometallics* **1999**, *18*, 2571.
(34) Crabtree, R. H.; Holt, E. M.; Lavin, M.; Morehouse, S. M. *Inorg. Chem.* **1985**, *24*, 1986.
(35) (a) Del Zotto, A.; Della Ricca, B.; Zangrando, E.; Rigo, P. *Inorg. Chim. Acta* **1997**, *261*, 147. (b) Del Zotto, A.; Mezzetti, A.; Rigo, P. *J. Chem. Soc., Dalton Trans.* **1994**, 2257.
(36) Günther, H. *NMR Spectroscopy: Basic Principles, Concepts, and Applications in Chemistry*, 2nd ed.; John Wiley & Sons: New York, 1995; Chapter 9.

Figure 3. ^{1}H NMR spectra of **1** in the *o*-methyl group region: experimental in CDCl₃ (left) and calculated (right).

Table 2. Rate Constants of the Xylyl Rotation for **1** in CDCl₃

temp (K)	k (s⁻¹)	temp (K)	k (s⁻¹)
262	22	306	424
273	55	317	698
284	120	327	1093
295	234		

the xylyl groups along the P−C bond. Line shape analysis of the spectra of Figure 3 allows the calculation of the rate constants at different temperatures (Table 2).

The Eyring plot of ln(*k/T*) vs 1/*T* is reasonably linear (Figure 4); thus the process obeys first-order kinetics. The derived activation parameters are $\Delta H^\ddagger$ = 9.6 ± 0.2 kcal/mol and $\Delta S^\ddagger$ = −15.4 ± 0.7 eu, which lead to $\Delta G^\ddagger$ = 14.2 ± 0.1 kcal/mol at 298 K. By changing the solvent to C₂D₂Cl₄, the coalescence temperature T_c becomes 45 °C with a slight increase of the free energy of activation, i.e., $\Delta G^\ddagger_{318}$ = 14.8 ± 0.2 kcal/mol ($\Delta\nu$ = 197 Hz).

The $\Delta H^\ddagger$ and $\Delta G^\ddagger$ values of **1** agree with those reported in the literature for the exchange process of agostic complexes,
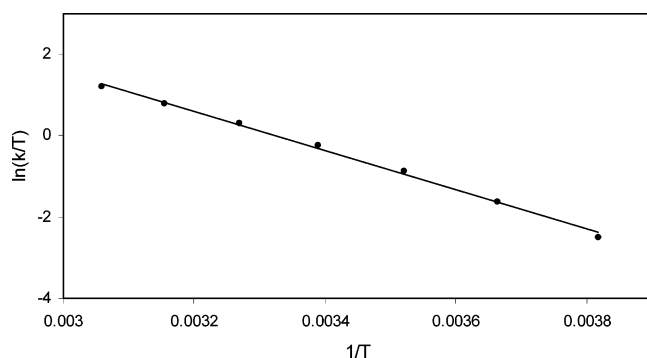
Figure 4. Eyring plot of the rate constants for the xylyl rotation in **1**.

indicating that **1** has a relatively high energy barrier of the xylyl rotation,[37] due to the cleavage of the ruthenium···methyl interaction (see later the computational DFT results) (Scheme 1). Interestingly, several complexes, which contain P(2-MeC$_6$H$_4$)$_3$, show a hindered rotation of the tolyl groups, as occurs for [Pt(2-CH$_2$C$_6$H$_4$)P(2-MeC$_6$H$_4$)$_2$-*C,P*](S$_2$CNMe$_2$) ($\Delta G^\ddagger_{318}$ = 15.2 kcal/mol),[38] Cr(C$_6$H$_6$)(CO)$_2$[P(2-MeC$_6$H$_4$)$_3$] ($\Delta G^\ddagger_{238}$ = 12.0 kcal/mol),[39] Cr(CO)$_5$[P(2-MeC$_6$H$_4$)$_3$] and Fe(CO)$_4$[P(2-MeC$_6$H$_4$)$_3$] ($\Delta G^\ddagger_{233}$ = 9.2 and 10.7 kcal/mol).[40] The relatively small negative $\Delta S^\ddagger$ value for **1** is probably associated with an intramolecular process, even though a weak interaction between the electron deficient metal center and the solvent at the transition state cannot be ruled out.[41] Note that the $\Delta S^\ddagger$ parameter is not always a reliable indicator of the mechanism since the solvent can affect its value even by 10 eu.[42] The negative $\Delta S^\ddagger$ for **1** could be indicative of a more ordered structure at the transition state being associated with the concerted rotations of the xylyl group and the other substituents of the two *cis* arranged phosphines. Consider in this respect the negative $\Delta S^\ddagger$ values (down to −18 eu) reported for the bulky phosphine complexes [Ir(H)$_2$LL$'_2$]$^+$ that undergo an intramolecular hydride exchange.[43]

As regards the stabilization of **1**, the two *o*-methyl groups of the xylyl seem to play an important role. Thus, all attempts to isolate an analogous complex from a phosphine ligand that carries only one *o*-methyl group, namely, the species RuCl$_2$-[PPh$_2$(2-MeC$_6$H$_4$)]$_2$, have failed. Furthermore, reaction of **1** with PPh$_2$(2-MeC$_6$H$_4$) in CDCl$_3$ leads to a reddish-brown solution that contains a mixture of RuCl$_2$[PPh$_2$(2-MeC$_6$H$_4$)]$_3$ (^{31}P NMR δ = 44.8, broad) and [RuCl$_2$\{PPh$_2$(2-MeC$_6$H$_4$)\}$_2$]$_2$ (δ = 64.0 and 55.7, $^2J_{PP}$ = 38.8 Hz). The latter result is inferred from the data relative to the complexes RuCl$_2$(PPh$_3$)$_3$ (δ 40.9 broad) and

[RuCl$_2$(PPh$_3$)$_2$]$_2$ (δ 58.3 and 53.0, J_{PP} = 41.5 Hz).[15a] No reaction of ethylene (1 atm) or THF with **1** has been observed in CDCl$_3$, the T_c not being significantly affected. Furthermore, ^{1}H NMR experiments carried out for complex **1** under high dihydrogen pressure (40 atm) show no appreciable effect, indicating that no formation of the dihydrogen complex of the type RuCl$_2$(H$_2$)L$_2$ (L = phosphine) occurs and that the δ-agostic Ru···H$_3$C interaction is stronger than any possible Ru···H$_2$ binding.

Reaction of 1 with NaX (X = I, OCN). In order to extend the number of isolable 14-electron ruthenium(II) complexes, we have prepared the derivatives RuX$_2$[PPh$_2$(2,6-Me$_2$C$_6$H$_3$)]$_2$ (X = I, **2**, NCO, **3**). It is well-known that ruthenium chloride complexes can be quantitatively converted into the corresponding halogenide or pseudohalogenide derivatives by reaction with the corresponding alkali metal salts.[44] Thus, treatment of **1** with an excess of sodium iodide in acetone at room temperature afforded the ruthenium iodide derivative, which analyzed (C, H, I) satisfactorily as RuI$_2$[PPh$_2$(2,6-Me$_2$C$_6$H$_3$)]$_2$ (**2**) by complete displacement of two chloride ligands (eq 1). In the solid state the dark brown complex **2** is thermally stable, and it can be kept in air for a long period without appreciable decomposition.

X	
I	**2**
NCO	**3**
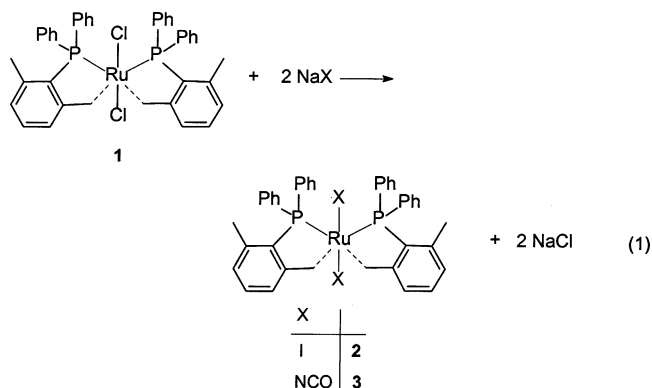
The ^{1}H NMR spectrum of **2** at 20 °C exhibits a doublet at δ 1.88 with a J_{HP} = 4.6 Hz for the two methyl groups close to the ruthenium center, whereas the signal at δ 1.30 corresponds to the noninteracting methyl groups. The variable temperature ^{1}H NMR spectra of **2** in C$_2$D$_2$Cl$_4$ show a fluxional process with a coalescence temperature at 75 °C and a $\Delta G^\ddagger_{348}$ of 16.6 ± 0.3 kcal/mol ($\Delta\nu$ = 116 Hz). At temperatures above 80 °C complex **2** begins to decompose with release of free phosphine and formation of uncharacterized products. In the ^{13}C NMR spectrum at 20 °C the noninteracting methyl groups appear at δ 24.0, whereas the pseudo triplet at δ 10.0 with $|^{trans}J_{CP} + {}^{cis}J_{CP}|$ = 24.4 Hz is due to the agostic methyls. The ^{1}H and ^{13}C NMR data for the *o*-methyls of **2** at room temperature are rather similar to those of **1** recorded at −50 °C. The higher barrier of rotation for **2** compared to that of **1** is likely to be ascribed to a stronger repulsion between the iodide and methyl group in the transition state.

Similarly to **2**, the red complex **3** was obtained by reaction of **1** with NaOCN in acetone at room temperature (eq 1). The ^{1}H and ^{13}C NMR data of **3** at room temperature resemble those of **1**, with the proton signal of the agostic methyl at δ 2.02 that

(37) Morse, P. M.; Spencer, M. D.; Wilson, S. R.; Girolami, G. S. *Organometallics* **1994**, *13*, 1646 and references therein.

(38) Forniés, J.; Martín, A.; Navarro, R.; Sicilia, V.; Villaroya, P. *Organometallics* **1996**, *15*, 1826.

(39) Howell, J. A. S.; Palin, M. G.; McArdle, P.; Cunningham, D.; Goldschmidt, Z.; Gottlieb, H. E.; Hezroni-Langerman, D. *Organometallics* **1993**, *12*, 1694.

(40) Howell, J. A. S.; Palin, M. G.; McArdle, P.; Cunningham, D.; Goldschmidt, Z.; Gottlieb, H. E.; Hezroni-Langerman, D. *Inorg. Chem.* **1991**, *30*, 4683.

(41) Negative values of entropy for conformational processes in polarizable solvents have been found when the polarity of the solute is much higher in the transition state than in the initial state (Sandström, J. *Dynamic NMR Spectroscopy;* Academic Press: New York, 1982; Chapter 7). For examples of coordination of halocarbons to a metal center see: (a) Huang, D.; Huffman, J. C.; Bollinger, J. C.; Eisenstein, O.; Caulton, K. G. *J. Am. Chem. Soc.* **1997**, *119*, 7398. (b) Huhmann-Vincent, J.; Scott, B. L.; Kubas, G. J. *J. Am. Chem. Soc.* **1998**, *120*, 6808. (c) Tellers, D. M.; Bergman, R. G. *J. Am. Chem. Soc.* **2001**, *123*, 11508. (d) Butts, M. D.; Scott, B. L.; Kubas, G. J. *J. Am. Chem. Soc.* **1996**, *118*, 11831.
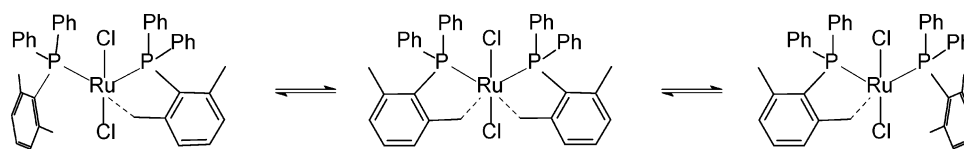
(42) (a) Kutal, C.; Sievers, R. E. *Inorg. Chem.* **1974**, *13*, 897. (b) Liu, L.; Guo, Q.-X. *Chem. Rev.* **2001**, *101*, 673. (c) Ruff, F. *J. Mol. Struct. (THEOCHEM)* **2002**, *617*, 31.

(43) Cooper, A. C.; Caulton, K. G. *Inorg. Chem.* **1998**, *37*, 5938.

(44) (a) Bennett, M. A.; Smith, A. K. *J. Chem. Soc., Dalton Trans.* **1974**, 233. (b) Wilczewski, T.; Bochénska, M.; Biernat, J. F. *J. Organomet. Chem.* **1981**, *215*, 87.

Scheme 1

splits into a doublet (J_{HP} = 4.3 Hz) at −40 °C. In the IR spectrum the NCO band of **3** is at 2239 cm^{-1}, in agreement with the other cyanato complexes that show coordination through the nitrogen donor atom.[45] So far, no examples of coordination through the oxygen have been reported in the literature for ruthenium cyanate complexes.[45a] In the formation of **2** and **3** the ^{31}P NMR spectra recorded during reactions showed resonances at δ 57.7 and 58.9, respectively. The latter occur between that of **1** and those of **2** and **3** and can be attributed to the formation of the intermediate monosubstituted complexes RuClX[PPh$_2$(2,6-Me$_2$C$_6$H$_3$)]$_2$ (X = I, NCO).

Complex **3** shows a fluxional behavior similar to that of **1** with a T_c of 30 °C (CDCl$_3$) that gives $\Delta G^\ddagger_{303}$ = 14.3 ± 0.2 kcal/mol ($\Delta\nu$ = 127 Hz). In conclusion, the 14-electron complexes **1** and **3** show rather similar free energy of activation, whereas the iodo derivative **2** displays the most hindered rotation of the xylyl group. This result also suggests that hydrogen bonding between the methyl and halogens is negligible[46] and that a major role is played by the agostic interaction and the bulkiness of the axial ligand.

Structural Survey of Complexes with Intra- or Intermolecular M···H$_3$C Interaction. Table 3 compares selected structural parameters of **1** with those of about forty X-ray structures of transition metal complexes that are deposited in the Cambridge Structural Database[22a] (version 5.24) and feature weak M···H$_3$C interactions.[22b] A more general structural analysis of the role of the metals in hydrogen bonding has recently appeared.[22c]

The search was based on the following criteria: (1) the CH$_3$ moiety is bound to an sp^3 or sp^2 carbon atom; (2) the transition metal belongs to groups 3−10; (3) no α-agostic case, with a direct M−CH$_3$ σ linkage, is taken into account because inconsistent with the first criterion; (4) the M···C separation is in the range 1.90−3.00 Å; (5) the intermediate atoms X$_\alpha$, Y$_\beta$, Z$_\gamma$, for γ through ε interactions are elements of groups 14−16 (Figure 5); (6) by following the criterion used by other authors

for a database survey of agostic compounds,[22b] any structural hit with R factor >7.5 is excluded from the statistical analysis (see footnote c in Table 3). Importantly, no neutron diffraction study is reported for any of the species complying with the above general criteria. Because X-ray data provide poor reliability for distances that involve the hydrogen atoms, the discussion will be mainly focused on the angular parameters. For any hit (refcode), Table 3 reports the type of connectivity, the nature of the unsaturated metal fragment, and the nature of the interconnecting chain. The M···C$_1$ and the three M···H distances (M···H$_1$ being the shortest one) are followed by three relevant angular values and by the dihedral angle between the planes M,C$_2$,C$_1$ and C$_2$,C$_1$,H$_1$ (i.e., the CH$_3$ torsion about the vector C$_1$−C$_2$). Finally, an index (defined in footnote a of Table 3) quantifies the puckering of the ring closed by the M···C$_1$ vector. While β species are trivially planar (index = 1), for higher connectivities the terminal C$_1$−C$_2$ vector can be significantly oblique with respect to the ring plane (index < 1). The scatter plot of Figure 6 relative to pure agostic compounds reveals a linear correlation between the angle M···C$_1$−C$_2$ and the rotation of the terminal CH$_3$ group. With a few outliers (to be discussed individually), the types of interaction fall in different zones. Thus, the angle M···C$_1$−C$_2$ and the dihedral angle M−C$_1$−C$_2$−H$_1$ increase synchronously in going from β to δ compounds. Questionably, the two known ε cases are associated with the most open M···C$_1$−C$_2$ angles and the smallest CH$_3$ torsions.

The average parameters for the different connectivities (including one intermolecular case) are also presented in Figure 5. It is possible to explain why the methyl torsion is practically 0° in the β species but increases progressively for the others. By assuming that in no case is the tetrahedral

(45) (a) Ragaini, F.; Longo, T.; Cenini, S.; Demartin, F. *J. Chem. Soc., Dalton Trans.* **1996**, 3221. (b) Bonfada, E.; Maichle-Mossmer, C.; Strähle, J.; Abram, U. *Z. Anorg. Allg. Chem.* **1999**, *625*, 1327. (c) Hansen, H. D.; Maitra, K.; Nelson, J. H. *Inorg. Chem.* **1999**, *38*, 2150. (d) Gül, N.; Nelson, J. H. *Organometallics* **1999**, *18*, 709. (e) Che, C. M.; Tang, W. T.; Lee, W. O.; Wong, W. T.; Lai, T. F. *J. Chem. Soc., Dalton Trans.* **1989**, 2011.
(46) (a) Steiner, T. *Angew. Chem., Int. Ed.* **2002**, *41*, 49. (b) Aullón, G.; Bellamy, D.; Brammer, L.; Bruton, E. A.; Orpen, A. G. *Chem. Commun.* **1998**, 653.
(47) Contreras, L.; Monge, A.; Pizzano, A.; Ruiz, C.; Sanchez, L.; Carmona, E. *Organometallics* **1992**, *11*, 3971.
(48) Carmona, E.; Sánchez, L.; Marín, J. M.; Poveda, M. L.; Atwood, J. L.; Priester, R. D.; Rogers, R. D. *J. Am. Chem. Soc.* **1984**, *106*, 3214.
(49) Jordan, R. F.; Bradley, P. K.; Baenziger, N. C.; LaPointe, R. E. *J. Am. Chem. Soc.* **1990**, *112*, 1289.
(50) Crowther, D. J.; Baenziger, N. C.; Jordon, R. F. *J. Am. Chem. Soc.* **1991**, *113*, 1455.
(51) Jordan, R. F.; LaPointe, R. E.; Bradley, P. K.; Baenziger, N. *Organometallics* **1989**, *8*, 2892.
(52) Hills, A.; Hughes, D. L.; Jimenez-Tenorio, M.; Leigh, G. J.; McGeary, C. A.; Rowley, A. T.; Bravo, M.; McKenna, C. E.; McKenna, M.-C. *J. Chem. Soc., Chem. Commun.* **1991**, 522.
(53) Wen, T. B.; Zhou, Z. Y.; Lau, C.-P.; Jia, G. *Organometallics* **2000**, *19*, 3466.
(54) (a) Feng, S. G.; White, P. S.; Templeton, J. L. *J. Am. Chem. Soc.* **1990**, *112*, 8192. (b) Feng, S. G.; White, P. S.; Templeton, J. L. *J. Am. Chem. Soc.* **1992**, *114*, 2951.

(55) Data are from Scherer et al.: Scherer, W.; Priermeier, T.; Haaland, A.; Volden, H. V.; McGrady, G. S.; Downs, A. J.; Boese, R.; Blaser, D. *Organometallics* **1998**, *17*, 4406. Other entries of this compound in the Cambridge Structural Database are as follows: (a) Dawoodi, Z.; Green, M. L. H.; Mtetwa, V. S. B.; Prout, K. *J. Chem. Soc., Chem. Commun.* **1982**, 802. (b) Cotton, F. A.; Petrukhina, M. A. *Inorg. Chem. Commun.* **1998**, *1*, 195. (c) Scherer, W.; Hieringer, W.; Spiegler, M.; Sirsch, P.; McGrady, G. S.; Downs, A. J.; Haaland, A.; Pedersen, B. *Chem. Commun.* **1998**, 2471. (d) Dawoodi, Z.; Green, M. L. H.; Mtetwa, V. S. B.; Prout, K.; Schultz, A. J.; Williams, J. M.; Koetzle, T. F. *J. Chem. Soc., Dalton Trans.* **1986**, 1629.
(56) (a) Jaffart, J.; Mathieu, R.; Etienne, M.; McGrady, J. E.; Eisenstein, O.; Maseras, F. *Chem. Commun.* **1998**, 2011. (b) Jaffart, J.; Etienne, M.; Maseras, F.; McGrady, J. E.; Eisenstein, O. *J. Am. Chem. Soc.* **2001**, *123*, 6000.
(57) Conroy-Lewis, F. M.; Mole, L.; Redhouse, A. D.; Litster, S. A.; Spencer, J. L. *Chem. Commun.* **1991**, 1601
(58) Fryzuk, M. D.; Johnson, S. A.; Rettig, S. J. *J. Am. Chem. Soc.* **2001**, *123*, 1602.
(59) Hay-Motherwell, R. S.; Wilkinson, G.; Hussain-Bates, B.; Hursthouse, M. B. *J. Chem. Soc., Dalton Trans.* **1992**, 3477.
(60) Hay-Motherwell, R. S.; Hussain-Bates, B.; Hursthouse, M. B.; Wilkinson, G. *J. Chem. Soc., Chem. Commun.* **1990**, 1242.
(61) Hay-Motherwell, R.; Wilkinson, G.; Sweet, T. K. N.; Hursthouse, M. B. *Polyhedron* **1996**, *15*, 3163.
(62) Binger, P.; Biedenbach, B.; Mynott, R.; Kruger, C.; Betz, P.; Regitz, M. *Angew. Chem., Int. Ed. Engl.* **1988**, *27*, 1157.
(63) Urtel, H.; Meier, C.; Eisentrager, F.; Rominger, F.; Joschek, J. P.; Hofmann, P. *Angew. Chem., Int. Ed.* **2001**, *40*, 781.
(64) Ong, C.; Kickham, J.; Clemens, S.; Guerin, F.; Stephan, D. W. *Organometallics* **2002**, *21*, 1646.
(65) Tenorio, M. J.; Mereiter, K.; Puerta, M. C.; Valerga, P. *J. Am. Chem. Soc.* **2000**, *122*, 11230.

Table 3. Structures that Feature Agostic (β, γ, δ, and ϵ Type) or Intermolecular $M\cdots H_3C$ Interactions[a]

| refcode and ref	type	metal	fragment type	connecting group $M\cdots CH_3$	$M–H_1$	$M–H_2$	$M–C_1$	$M–C_1–C_2$	$C_1–M–H_1$	$M–C_2–C_1–H_1$	puckering index
KUYSUS[47]	β	Mo(II)	ML_6 (ps oct)	$-C(O)-$	2.57	>3	2.76	47	21	4	1.00
BOLCIO[48]	β	Mo(II)	ML_6 (ps oct)	$-C(O)-$	2.06	>3	2.60	52	21	6	1.00
JECKUX[49]	β	Zr(IV)	MCp_2L_2	$-CH_2-$	2.16	>3	2.52	60	20	1	1.00
KIMZOV[50]	β	Zr(IV)	MCp_2L	$-C(=CR2)-$	2.29	>3	2.70	54	20	2	1.00
SEHZUA[51]	β	Zr(IV)	MCp_2L_2	$-C(=CR2)-$	2.32	>3	2.72	55	20	10	1.00
KIRFOG[52]	β	Fe(II)	MCp_2R	$-C(=CR2)-$	1.77	2.82/2.91	2.20	60	30	5	1.00
RAHMUI[53]	β	Os(II)	ML_5 (sq.pyr.)	$-C(=CR2)-$	1.81	>3	2.53	53	27	2	1.00
SIMLOP[54]	β	W(II)	ML_6 (ps oct)	$=C(Ph)-$	2.11	>3	2.48	52	22	0	1.00
BIXFUJ[55]	β	Ti(IV)	ML_6 (ps oct)	$-CH_2-$	2.06	>3	2.50	59	23	1	1.00
JOWLAI[56a]	β	Nb(III)	ML_6 (ps oct)	$-CHR-$	2.17	>3	2.61	59	25	2	1.00
AFIGEB[56b]	β	Nb(III)	ML_6 (ps oct)	$-CHR-$	2.13	>3	2.59	59	23	1	1.00
KOKTAF[57]	β	Ni(II)	ML_3 (T shape)	$-CH_2-$	1.64	2.62/2.78	2.08	64	29	1	1.00
UDICIT[58]	β	Ta(III)	ML_5 (ps oct)	$-CH_2-$	2.08	>3	2.50	63	23	10	1.00
JURLUD[59]	γ	Ir(III)	ML_3 (trig pyr) 3 CH_3 fac	$-(o\text{-aryl})-$	2.28	>3	2.87	72	17	16	0.999
					2.36	>3	2.91	70	17	13	1.000
					2.39	3.16	2.90	72	18	25	1.000
VEZNIX[60]	γ	Rh(III)	ML_3 (trig pyr) 3 CH_3 fac	$-(o\text{-aryl})-$	2.24	2.90	2.79	72	20	6	1.000
					2.36	2.80	2.79	72	21	25	1.000
					2.30	3.08	2.78	72	17	27	1.000
RUFFON[61]	γ	Ni(II)	ML_3 (T shape) 2 CH_3 equat	$-(o\text{-aryl})-$	2.24	>3	2.89	70	17	6	0.997
					2.28	>3	2.88	70	20	15	0.998
SAKWUW[62]	γ	Rh(III)	ML_5 (sq pyr)	$-C(=P-)-CR_2-$	2.73	2.73	2.98	76	21	57	1.000
QIVHEI[63]	γ	Rh(I)	ML_3 (T-shape)	$-CH_2-CR_2-$	2.20	2.27	2.49	85	23	58	1.000
MITSEN[64]	γ	Ti(IV)	ML_4 (tetr)	$-S-CR_2-$	2.36	2.64	2.89	106	20	51	0.999
HITGIA[24]	γ	Ru(II)	ML_5 (sq pyr)	$-PR_2-CR_2-$	2.29	>3	2.94	88	16	33	0.966
QODDES[65]	γ	Ru(II)	ML_5 (sq pyr)	$-PR_2-CR_2-$	2.26	>3	2.95	85	18	29	0.924
DAKHAY[34]	δ	Ir(III)	ML_5 (sq pyr)	$-8,Metquinol.-$	2.08	2.39	2.69	100	18	43	1.000
WURJAU[6]	δ	Pt(II)	ML_3 (T shape)	$-PR_2-(o\text{-aryl})-$	2.06	2.08	2.43	113	22	59	1.000
HANWEY[66]	δ	Ir(III)	ML_5 (sq pyr)	$-CR=CR-CR_2-$	2.31	2.33	2.70	105	23	59	1.000
[b]GOYGOQ	δ	Ru(II)	ML_4 (butterfly)	$-PR_2-(o\text{-aryl})-$	2.20	2.33	2.65	107	23	55	0.990
					2.18	2.30	2.65	107	23	53	0.990
present complex **1**	δ	Ru(II)	ML_4 (butterfly) 2 CH_3 cis	$-PR_2-(o\text{-aryl})-$	2.14	2.39	2.63	108	24	56	0.989
					2.11	2.49	2.66	106	24	52	0.992
FEQGEN[67]	δ	Cr(II)	ML_4 (sq pl) 2 CH_3 trans	$-NR-(o\text{-aryl})-$	2.08	2.50	2.63	98	23	46	0.965
					2.08	2.50	2.63	98	23	46	0.965
DOZYUM[68]	δ	Co(II)	ML_3 (trig pl) 2 CH_3 trans	$-O-CR_2-CR_2-$	2.22	2.70	2.79	95	21	47	0.973
					2.43	2.64	2.88	98	21	55	0.971
JOJYIQ[26]	δ	Ru(II)	ML_5 (sq pyr) dimer	$-CR_2-PR_2-CR_2-$ 1 CH_3 per M	1.90	2.56	2.51	113	21	44	0.954
					1.88	2.52	2.51	113	22	46	0.953
[c]LOQJOQ[33b]	δ	Ru(II)	ML_5 (sq pyr)	$-(o\text{-pyraz})-CR_2-$	1.84	2.79	2.63	104	18	32	0.979
YITXAA[69]	δ	Fe(II)	ML_2 (linear) 2 CH_3 trans	$-(o\text{-aryl})-CR_2-$	2.17	2.55	2.73	102	22	48	0.998
					2.23	2.62	2.79	102	21	47	0.998
ZEPROB[69a]	δ	Mn(II)	ML_2 (linear) 2 CH_3 trans	$-(o\text{-aryl})-CR_2-$	2.27	2.56	2.78	102	22	51	0.997
					2.29	2.50	2.77	103	22	53	0.997
[c]YUWBUN[70]	δ	Pd(II)	ML_3 (sq pl)	$=CR-NR-CR_2-$	2.40	2.82	2.99	99	19	46	0.990
UDUKAF[71]	δ	Ru(II)	ML_5 (sq pyr) 2 ind mol	$-(o\text{-Si}-N$ hetero-cycle)$-CR_2-$	2.33	2.64	2.90	113	20	49	0.996
					2.35	2.66	2.91	112	20	50	0.998
VIVDEJ[72]	δ	Ti(III)	ML_3 (trig pyr) dimer	$-N_{bridg}-Si-CR_2-$ 1 CH_3 per M	2.10	2.61	2.75	112	20	42	0.969
					2.17	2.63	2.79	112	20	44	0.971
[c]KIRMAZ[73]	ϵ	Mn(II)	ML_3 (trig pl) dimer	$-S_{br.}-(o\text{-aryl})-CR_2-$ 1 CH_3 per M	1.99	>3	2.92	119	6	5	0.940
					1.99	>3	2.92	119	6	5	0.940
KIRMED[73]	ϵ	Fe(II)	ML_3 (trig pl) dimer	$-S_{br.}-(o\text{-aryl})-CR_2-$ 1 CH_3 per M	1.79	>3	2.72	118	6	6	0.942
					1.79	>3	2.72	118	6	6	0.942
[c]ROGBIY[2a]	inter-molecule	Fe(II)–porphyrin	ML_4–heptane disordered				2.5–2.8	na			
EFOWIF[74]	inter-molecule	Rh(II) dimer	$M_2(acet)_4$ 2 axial CH_3		2.18	2.59/3.07	2.74	148	21	36	
					2.46	2.66/2.79	2.80	169	23	25	

[a] The metal belongs to groups 3–10, whereas the terminal CH_3 group is bound to a carbon atom with sp^3 (alkyl-like) or sp^2 (aryl-, vinyl-, or acyl-like) hybridization. The vector $M\cdots H_3C$ closes a ring of variable size, for which a puckering index is defined as $\sum_i \alpha_i/((n-2)\times 180)$. [b] The structure GOYGOQ refers to the X-ray determined structure of the present complex **1**.[5] [c] The structure is not considered for the statistical analysis (see text and Figure 6) because the final R factor is >7.5.

geometry of the C_1 atom significantly affected by the interaction with the metal, only the β complexes allow the $C_1–H_1$ bond to lie in the M,C_2,C_1 plane and the $M\cdots C_1$ vector to bisect the angle $C_2–C_1–H_1$. Thus, the sum of the angles $M\cdots C_1–C_2$ and $M\cdots C_1–H_1$ (averages of 57(5)° and 53(7)°, respectively) almost matches the ideal 109.47° value. This allows the bond $C_1–H_1$ to lie in the M,C_2,C_1 plane and the $M\cdots C_1$ vector to almost bisect the angle $C_2–C_1–H_1$. Moreover, the angle subtended at the metal by the $C_1–H_1$ bond is sufficiently large for efficient

$M\cdots\eta^2$-HC coordination (the range 20°–30° seems to be optimal). Were the CH_3 group rotated by 60° about the bond $C_1–C_2$ (to simulate the nonclassical $M\cdots\eta^3$-H_2C coordination), the two shorter $M\cdots H$ distances would become too large to be consistent with any agostic character.

For higher connectivities, larger $M\cdots C_1–C_2$ angles imply out of plane rotation of the CH_3 group. In the γ complexes the $M\cdots C_1–C_2$ angle is about 17° more open than in the β species (with the exception of MITSEN),[64] and the four-membered ring
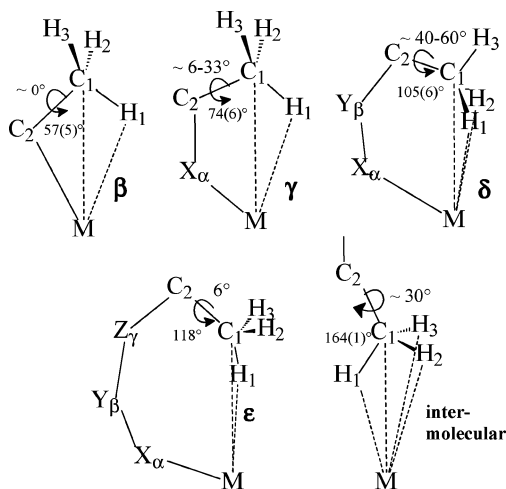
Figure 5. Summary of the geometrical parameters that define the stereochemistry of the C—CH$_3$ moiety in the agostic (β through ϵ) and in the intermolecular cases.
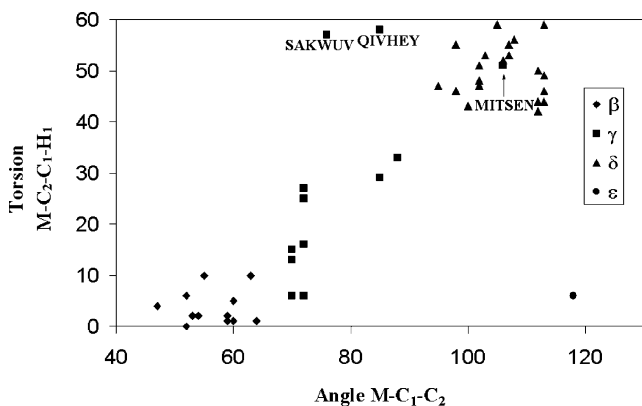
Figure 6. Scatter plot showing the essentially linear relationship between the opening of the M$\cdots$C$_1$—C$_2$ angle and the torsion of the CH$_3$ group about the C$_1$—C$_2$ bond.

is generally planar (in six out of the eight cases, the puckering index is ~1). Were the bond C$_1$—H$_1$ also to lie in the ring, the distance M$\cdots$H$_1$ would be too short and the angle C$_1\cdots$M$\cdots$H$_1$ too closed (<20°) for an efficient donation of the C$_1$—H$_1$ electron density. The system reacts by a limited rotation of the methyl group as inferred from the M—C$_2$—C$_1$—H torsion angles in the range 0—30°. However, the values are surprisingly close to 60° for the species SAKWUW,[62] QIVHEY,[63] and MITSEN[64] (see Figure 6). Concerning the first two cases, an alternative interpretation of the structural data allows the dismissal of the outlier character, and it is presented as Supporting Information. The compound MITSEN, shown in Figure 7, is the only example of an early transition metal in Table 3 and is peculiar in being a γ complex falling in the middle of the δ zone in Figure 6. In fact, the open Ti$\cdots$C$_1$—C$_2$ angle of 105.6° accompanies a CH$_3$ torsion of 51°. The agostic interaction in MITSEN was not described by the authors who considered the complex authentically tetrahedral as other Ti(IV) phosphinimide—thiolate compounds (e.g., Ti(NP^{t}Bu$_3$)$_2$(SCH$_2$Ph)$_2$) reported in the same paper.[64] In contrast, the TiN$_2$S$_2$ coordination sphere is evidently distorted toward a trigonal pyramid together with a significant squeezing of the agostic four-membered ring. This is indicated by the 85° Ti$\cdots$C$_1$—C$_2$ angle that is at about 20° more closed than the equivalent angle at the other thiolate ligand (see Figure
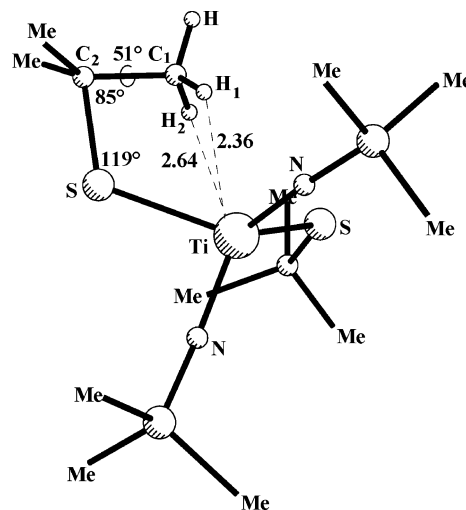
Figure 7. Molecular structure of the γ agostic complex MITSEN.[64]

7). Due to the geometric deformation, this γ species is uniquely close to M$\cdots\eta^3$-H$_2$C coordination.

In δ agostic complexes, the dihedral angle M—C$_2$—C$_1$—H is generally larger than 40°. The torsion angle shown by the neutron diffraction study of **1** (54°) indicates that M$\cdots\eta^3$-H$_2$C coordination is almost attained, whereas the classical M$\cdots\eta^2$-HC coordination would cause an unrealistically small Ru$\cdots$H distance (1.7 Å) and C$_1\cdots$Ru$\cdots$H$_1$ angle (4°). Very far from the classical model are the 14-electron platinum(II) complex [Pt(P-C){PCy$_2$(2,6-Me$_2$C$_6$H$_3$)}]$^{+}$ [6] and the species [Ir(H)(PMe$_3$)$_3${C(=CH^{t}Bu)(C$_4$H$_4$O)}]$^+$ (HANWEY).[66] In both cases, the methyl torsion is near to 60° with two fairly similar M$\cdots$H distances (see Table 3), the metals lying out of the CH$_2$ plane (the dihedral angle M—H$_1$—H$_2$—C$_1$ is 152° and 154° for the Pt and Ir complex, respectively). This occurs because the M$\cdots$C$_1$—C$_2$ angle (113° and 105°, respectively) cannot open up to the ideal 125° value that was optimized for intermolecular metal—alkane adducts.[3] In contrast, a longer pendant chain as in the ϵ species allows to get closer to the latter limit (about 119°, as reported in Figure 5).

Unexpectedly, only one well-characterized ϵ compound, namely, [Fe{S(C$_6$H$_2^t$Bu$_3$)}$_2$]$_2$ (KIRMED[73]), is reported to have the classical M$\cdots\eta^2$-H$_2$C coordination and is the most evident outlier in Figure 6 with a C$_1$—M—H$_1$ angle of only 6° and a very short Fe$\cdots$H distance (1.79 Å). On the basis of the arguments discussed, ϵ complexes should adopt a conformation with a 60° rotation of the methyl group. Calculations on KIRMED give two almost equal short Fe$\cdots$H separations (about 2.31 Å), with an agostic interaction quite similar to that computed for the metal—alkane adducts with ideal M$\cdots\eta^3$-H$_2$C coordination.[3]

Finally, we point out a well-documented case of M$\cdots$H$_3$C intermolecular interaction. At variance with ROGBIY, the poorly

(66) Selnau, H. E.; Merola, J. S. *Organometallics* **1993**, *12*, 3800.
(67) Gibson, V. C.; Newton, C.; Redshaw, C.; Solan, G. A.; White, A. J. P.; Williams, D. J. *J. Chem. Soc., Dalton Trans.* **1999**, 827.
(68) Olmstead, M. M.; Power, P. P.; Sigel, G. *Inorg. Chem.* **1986**, *25*, 1027.
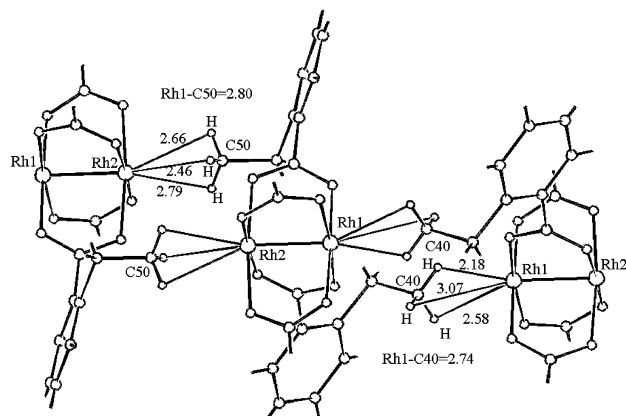(69) (a) Wehmschulte, R. J.; Power, P. P. *Organometallics* **1995**, *14*, 3264. (b) Muller, H.; Seidel, W.; Gorls, H. *Angew. Chem., Int. Ed. Engl.* **1995**, *34*, 325.
(70) Reger, D. L.; Collins, J. E. *J. Organomet. Chem.* **1995**, *491*, 159.
(71) Amoroso, D.; Haaf, M.; Yap, G. P. A.; West, R.; Fogg, D. E. *Organometallics* **2002**, *21*, 534.
(72) Cummins, C. C.; Schaller, C. P.; Van Duyne, G. D.; Wolczanski, P. T.; Chan, A. W. E.; Hoffmann, R. *J. Am. Chem. Soc.* **1991**, *113*, 2985.
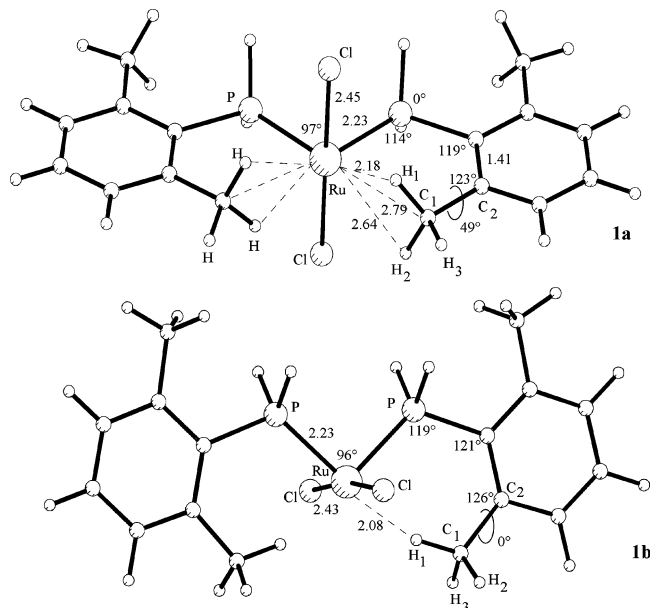(73) Power, P. P.; Shoner, S. C. *Angew. Chem., Int. Ed. Engl.* **1991**, *30*, 330.

Figure 8. Intermolecular Rh⋯H₃C interactions in the complex EFOWIF.[74]

Figure 9. Structural optimizations of RuCl₂[PH₂(2,6-Me₂C₆H₃)]₂. The model **1a** (top) is a stationary point calculated with C_2 symmetry. The C_{2v} model **1b** (bottom) is characterized by two imaginary frequencies that indicate vibration of the C_1–H_1 bonds off the main molecular plane.

defined adduct between an iron(II)−porphyrin complex and an *n*-heptane molecule,[2] the intermolecular M⋯H₃C interactions between the dimers Rh₂(μ-O₂CC₆H₂^iPr₃)₄ (EFOWIF) are evident.[74] While the authors described the system as an unprecedented example of a dirhodium tetracarboxylate complex with no axial coligands, the Rh⋯H₃C intermolecular interactions, roughly collinear with the Rh−Rh bond, were not discussed. Looking at the packing diagram of Figure 8, the significantly large Rh⋯C_1−C_2 angles (148° and 169° at the agostic atoms C40 and C50, respectively) are clearly indicative of a not previously reported M⋯η^4-H₃C coordination where the metal projects roughly over the tetrahedral face of the methyl group. This may be a consequence of the peculiar crystal packing, but the problem would deserve specific theoretical attention.

In closing the present section, we draw brief conclusions. In the β agostic complexes, the sp³ character of the alkylic carbon atom is fully consistent with the metal lying in the C_2,C_1,H_1 plane. Together with the α compounds, these species represent the most classical form of M⋯η^2-HC interaction. When the angle M⋯C_1−C_2 is larger than 55° (γ through ϵ cases), rotation of the methyl group about the C_1−C_2 bond is forced so that the hydrogen atom closest to the metal slips off the M,C_1,C_2 plane. Such a rotation is progressively larger (<30° for the γ complexes, >30° for the δ ones) but, even at the 60° limit, the connectivity between the metal and the agostic methyl group does not allow the metal to attain ideal M⋯η^3-H₂C coordination. The latter (metal coplanar with CH₂) is featured only by intermolecular adducts between a transition metal fragment and an alkane, provided that a peculiar packing mode does not favor an alternative arrangement, such as the quasi M⋯η^4-H₃C coordination in EFOWIF.[74]

Computational Analysis

DFT calculations have been performed to explore the electronic interactions occurring in **1** between the d⁶-L₄Ru(II) fragment and two agostic methyl groups at the empty octahedral *cis* coordination sites. To make complete structural optimization affordable, the phenyl substituents were omitted and the model RuCl₂[PH₂(2,6-Me₂C₆H₃)]₂ (**1a**) with C_2 symmetry was adopted. The computed geometry (upper part of Figure 9) agrees reasonably well with the experimental one (see also Table 1) as indicated, for instance, by the Ru−P bonds [2.23 Å vs 2.249-

(74) Cotton, F. A.; Hillard, E. A.; Murillo, C. A. *J. Am. Chem. Soc.* **2002**, *124*, 5658.

(7) Å (av)] and the Ru−Cl ones [2.45 Å vs 2.402(5) Å]. Also, the trends for the agostic methyl groups are consistent. The CH₃ torsion of 49° is slightly smaller than the experimental one (average value 54°), whereas the C−H bonds involved in metal interactions are consistently elongated (1.11 vs 1.09 Å). Correspondingly, the H−C−H angle that fixes the Ru⋯η^3-H₂C coordination mode is more open than its analogues (by at least 5°).

However, the lack of the phenyl rings has some consequences for the geometry of the model. Thus the 20° twisting of the xylyl groups, observed in **1**, is not reproduced in **1a**, where the xylyl substituents lie in the RuP₂ plane. The absence of steric hindrance affects other angular parameters as well. For instance, the angle P−Ru−P is smaller in **1a** than in **1** [97° vs 101.6(2)°], whereas the Cl−Ru−Cl is more open [176° vs 167.7(2)°] because the chlorine atoms bend away from the phenyl groups when they are present. Finally in the agostic backbone, the angle Ru−P−C_ipso is about 5° more open in **1a** than in **1** [114° vs 109.2(2)°] so that the computed Ru⋯H₃C interactions appear weaker than in the experiment. As a consequence, the Ru⋯C_1 separations are ca. 0.14 Å longer in **1a** than in **1** and so are the computed Ru⋯H₁, Ru⋯H₂ distances (2.18/2.64 Å in **1a** vs 2.14(1)/2.40(1) and 2.11(1)/2.51(1) Å in **1**). In this respect, it is worth recalling that a mixture of QM/MM calculations on the 14-electron species [Ir(H)₂-(P^tBu₂Ph)₂]⁺ showed significant shortening of the M⋯H distances upon the introduction of bulky substituents at the arm connecting the metal and the agostic group.[20]

Useful chemical hints can be drawn from the reproducibility of the Ru⋯η^3-H₃C interactions in the model. For instance, the angle Ru⋯C_1−C_2 and the methyl torsion are confirmed to have the expected values for δ species (107° and 49°, respectively), as inferred from their correlation. While the classical M⋯η^3-H₂C agostic type is confirmed in **1a**, the C_{2v} model complex **1b**, forced to have one C−H linkage per methyl group in the RuP₂ plane, does not optimize as a stationary point (see Figure
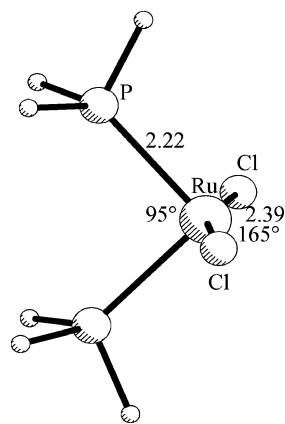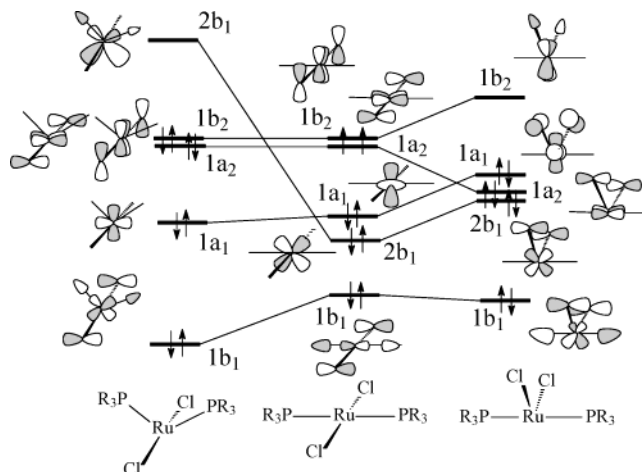
Figure 10. Optimized structure of $RuCl_2(PH_3)_2$.

9). The computed frequencies have two imaginary values that correspond to conrotatory and disrotatory out of plane movements of the two CH_3 groups. Obviously, these vibrations need not be synchronized and the actual transition state is attained when only one C–H bond passes through the RuP_2 plane. The energy of **1b** allows one to estimate a barrier of about 3.4 kcal mol^{-1} for single CH_3 rotation. The low value is consistent with the NMR data for **1**: i.e., the *o*-methyl rotation cannot be frozen out even at temperatures as low as -120 °C. Also, the geometry of **1b** shows that, at the TS structure, all of the angles of the MPC=C–CH_3 chain open up a few degrees to allow a reasonably long Ru···H_1 distance (2.08 Å). Importantly, the angle subtended at the metal by the C_1–H_1 bond is as small as 7°. This reduces the C–H electron density donated to the metal as confirmed by the computed metal charge. The latter is smaller by about 0.2 electrons in **1b** than in **1a**. Similar conclusions were reached by the NMR and theoretical study of aryl–bicycloheptylpalladium unsaturated systems, which are important intermediates in C_{aryl}–H catalytic activation through palladacycles.[76] In that case also, the model complex, where the C_{aryl}–H bond is coplanar with the unsaturated $L_3Pd(II)$ fragment, corresponds to a transition state and not to a stationary one.

Another interesting question concerns the degree of stabilization of the 14-electron $L_4Ru(II)$ system due to the agostic interactions. It is worth recalling that the four-coordinate complexes $[RuPh(CO)(P^tBu_2Me)_2]^+$ [19] or $[Ir(H)_2(P^tBu_2Ph)_2]^+$,[77] unlike **1**, have *trans*, rather than *cis*, phosphine ligands. Conversely, even the simplest C_{2v} complex $RuCl_2(PH_3)_2$ is optimized as a stationary point with *cis* structure (Figure 10), independently of the starting geometry.

Simple qualitative MO arguments (based on the EHMO method)[78] account easily for the preferred *cis* arrangement of the phosphine ligands in the presence of two chloride π donors. The energy stabilization with respect to the *trans* model complex is large (about 13 kcal mol^{-1}); moreover, the interconversion between the two conformers implies a change of the ground
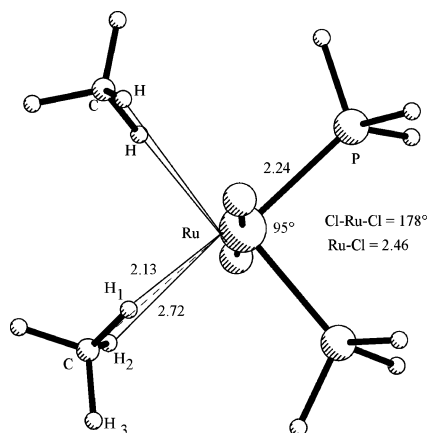
(75) Dunitz, J. D. *X-ray Analysis and the Structure of Organic Molecules*; Cornell University Press: Ithaca, NY, 1979 (referenced in the Supporting Information).
(76) Catellani, M.; Mealli, C.; Motti, E.; Paoli, P.; Perez-Carreño, E.; Pregosin, P. S. *J. Am. Chem. Soc.* **2002**, *124*, 4336.
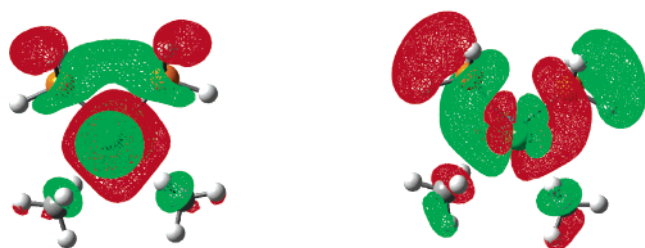(77) (a) Ujaque, G.; Cooper, A. C.; Maseras, F.; Eisenstein, O.; Caulton, K. G. *J. Am. Chem. Soc.* **1998**, *120*, 361. (b) Cooper, A. C.; Clot, E.; Huffman, J. C.; Streib, W. E.; Maseras, F.; Eisenstein, O.; Caulton, K. G. *J. Am. Chem. Soc.* **1999**, *121*, 97.
(78) (a) Hoffmann, R.; Lipscomb, W. N. *J. Chem. Phys.* **1962**, *36*, 2872. (b) Hoffmann, R.; Lipscomb, W. N. *J. Chem. Phys.* **1962**, *37*, 3489. (c) Mealli, C.; Proserpio, D. M. *J. Chem. Educ.* **1990**, *67*, 399.

Figure 11. Correlation diagram for the frontier levels of the d^6 species $RuCl_2(PR_3)_2$. The lowest filled MO $1b_1$ is ligand-based, and it is depicted to show its important role for the energetics of the rearrangement.

state for the square planar structure. This is highlighted by the correlation diagram of Figure 11 that shows how the d^6 metal center would adopt the triplet state at the latter geometry due to the quasi degeneracy of the $1a_2$ and $1b_2$ MOs (xz and yz) destabilized by the orthogonal p_π orbitals of both chloride ligands. Recently, the stability of the square planar triplet state has been experimentally and computationally ascertained for the Ru(II) complex $Ru[(^tBu_2PCH_2SiMe_2)_2N]Cl$.[12] In this case, the two SOMOs are found to be z^2 and yz as the nitrogen donor has only one p_π orbital donor.

As typical of butterfly fragments, the metal features, at both sides of Figure 11, a high lying σ metal hybrid orbital (not shown) and a d_π LUMO. The combination of the empty hybrid orbitals determines the double unsaturation of the 14-electron unit. The preference for the singlet isomer with a *cis* phosphine arrangement can be ascribed to two different factors. First of all, a larger HOMO–LUMO gap in the *cis* structure is attributable to strong σ-donor power of the phosphine ligands and to the high destabilization of the d_π level.

The second effect is to be related to the four electron repulsion between a RuP_2 bonding level and a combination of filled chloride p_π orbitals (compare in Figure 11 the energies of $1b_1$ along the interconversion pathway). Were hydride or CO ligands in the place of the chlorine atoms, the effect would be null or stabilizing, respectively. Accordingly, $1b_1$ is decisive for the complex geometry and the *cis* isomer of $RuCl_2(PH_3)_2$ is eventually favored.

As an extension, we have tried to optimize the structure of the adduct between $RuCl_2(PH_3)_2$ and two methane molecules. Figure 12 presents the C_2 structure of $RuCl_2(PH_3)_2(\eta^3-H_2CH_2)_2$ that is found to be a stationary point.

As reported by several other authors, in the methane adducts the interactions are essentially of the type M···η^3-H_2C.[3] Notice, in particular, that the angle formed at the carbon atom by the metal and the away-pointing H_3 atom is about 125°, i.e., the ideal value for the metal to lie in the CH_2 plane. Still, the two shortest Ru···H_1 and Ru···H_2 separations are rather asymmetric (2.13 and 2.72 Å, respectively). In our case, the binding energy for a single CH_4 molecule is computed to be small (3 kcal mol^{-1}) and less pronounced than that found by other authors for different metal adducts by using different levels of theory.[3d]

Figure 12. Optimized structure for $RuCl_2(PH_3)_2(\eta^3\text{-}H_2CH_2)_2$.

Figure 13. LUMO + 1 and LUMO of the complex $RuCl_2(PH_3)_2(\eta^3\text{-}H_2CH_2)_2$ modeled with two symmetrically arranged methane molecules.

Nonetheless, we have tried to focus on the nature of such weak chemical bonding.

First, we have calculated a single point where the two CH_4 molecules have been rotated to symmetrize the two shorter $Ru\cdots H$ distances. This has the minimum energy cost of only 0.7 kcal mol^{-1} that confirms the extremely flat potential energy surface for the interaction of the alkane. An insignificant barrier of 0.1 kcal mol^{-1} was found also by Koga and Morokuma for the same CH_4 rearrangement in the $RhCl(PH_3)_2(CH_4)$ fragment.[3c] Figure 13 presents the LUMO + 1 and LUMO for the ideally symmetric $M\cdots\eta^3\text{-}H_2C$ coordination in $RuCl_2(PH_3)_2$-$(\eta^3\text{-}H_2CH_2)_2$. Interestingly, the drawings of these antibonding levels highlight the major contribution of the methane carbon atoms in electron donation to the metal σ and d_π hybrid orbitals. Also when the $M\cdots\eta^3\text{-}H_2C$ coordination becomes asymmetric, there remains evidence for the contribution of the carbon p orbital with a slightly increased percentage of the hydrogen s orbitals.

The NMR study of **1** revealed that a rotation of the two xylyl groups about the P$-$C$_{ipso}$ vectors occurs in solution with a rotational barrier of 9.6 kcal mol^{-1}, indicating a significantly hindered process. Therefore, we have attempted to simulate the rotational mechanism also computationally. In order to speed up the search for the transition state, the model complex **1a** was further simplified by replacing one xylyl with a $-CH=CH-CH_3$ group, namely, $RuCl_2[PH_2(2,6\text{-}Me_2C_6H_3)][PH_2CH=CHCH_3]$. Three optimized structures are reported in Figure 14, with the xylyl group in the equatorial plane **1c**, or upright **1d** or at an intermediate orientation **TS**.

The loss of negative metal charge in **1d** (-0.70) and in **TS** (-0.76) compared to **1c** (-1.03) confirms that the agostic interaction is dative. However, the associated loss of energy is in any case very small, the ΔE between **1c** and **1d** being less

than 1 kcal mol^{-1}, whereas the **TS** barrier is estimated as 3.8 kcal mol^{-1}. In the structure **1d** with the upright xylyl group, the loss of the agostic interaction seems to be partially compensated by two Cl$\cdots$H$-$C hydrogen bonds, which are highlighted in Figure 14. The destabilization of the **TS** is most likely attributable to the loss of any attractive force, although, in the real system **1**, the steric hindrance of the phenyl substituents can be essential in hindering the xylyl rotation.

Conclusions

The present study has carefully analyzed, through experimental and theoretical approaches, a new class of 14-electron ruthenium(II) complexes that receive extra stability from two agostic interactions between the unsaturated metal center and the *o*-methyl groups of two phosphine xylyl substituents. The accurate location of the hydrogen atoms through a neutron diffraction study of **1** has allowed a unique and reliable interpretation of the stereochemical features. In particular, the nonclassical agostic interaction, where a whole CH_2 group acts as a donor in place of the single C$-$H bond ($M\cdots\eta^3\text{-}H_2C$ vs $M\cdots\eta^2\text{-}HC$ coordination), has been definitely established. Further evidence comes from the NMR studies of **1**$-$**3** that show that the $M\cdots\eta^3\text{-}H_2C$ interaction determines an upfield shift of the agostic carbon atoms, whereas the protons are at low field. In solution, **1**$-$**3** show a dynamic process that exchanges the *o*-methyl groups and the ^{1}H NMR line shape analysis for **1** is clearly indicative of a relatively strong agostic interaction.

In order to compare our experimental results with those already present in the literature, we made a survey of all the structures, deposited in CSD, that feature either agostic or intermolecular $M\cdots H_3C$ interactions. A linear correlation is found between the angle at the methyl carbon atom and the CH_3 torsion itself in relation to the different type of metal$\cdots$methyl connectivity.

DFT calculations have confirmed the preference for the nonclassical agostic interaction in a simplified model of **1**. A qualitative rationale for the stability of the 14-electron complex $RuCl_2(PR_3)_2$ with the *cis*-phosphine arrangement has been presented even in the absence of any agostic interaction. The bonding capability of this metal fragment toward CH_4 has been illustrated, and this study indicates the major involvement of one carbon p orbital in the nonclassical $M\cdots\eta^3\text{-}H_2C$ agostic interaction. Finally, an attempt has also been made to reconstruct computationally the dynamic behavior of the xylyl group as detected from the NMR measurements. By using an extremely simplified model, interesting trends have emerged, even though the experimental data are not matched precisely. In this context, the major role played in the real structure by the bulky phenyl substituents at the phosphorus atoms becomes most evident.

In summary, these studies have led to the following important conclusions. Whenever an attractive intermolecular interaction between an unsaturated metal center and an alkane CH_3 group is established, the $M\cdots\eta^3\text{-}H_2C$ coordination mode is preferred, most likely because one carbon p orbital points directly to the metal (see Figure 13). In one case, even a $M\cdots\eta^4\text{-}H_3C$ interaction mode has been documented, but this is probably due to a peculiar packing effect. Conversely, if there are links between the CH_3 group and the metal center, the interaction type depends on the length of the joining chain and, if the latter is particularly short, only the $M\cdots\eta^2\text{-}HC$ coordination mode is
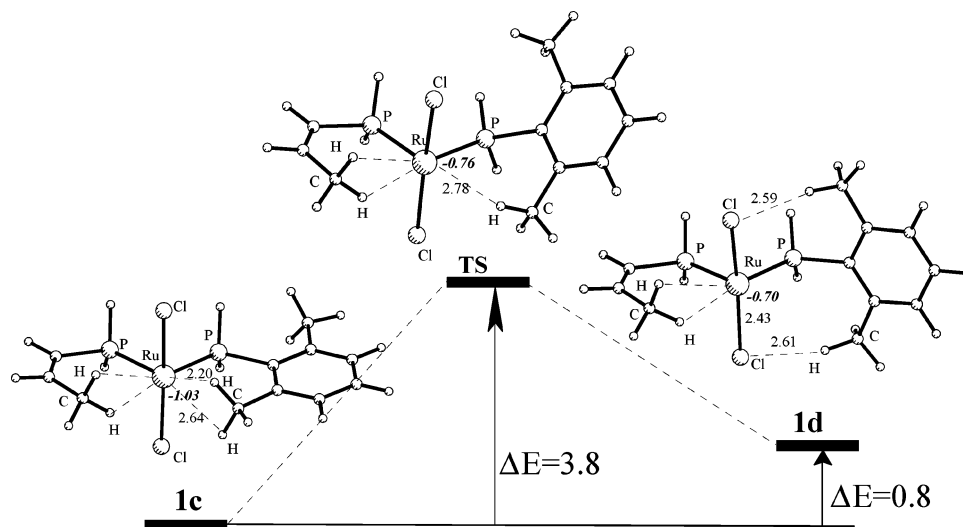
Figure 14. Modeling of the rotation of one xylyl group about the P−C$_{ipso}$ bond in the simplified model RuCl$_2$[PH$_2$(2,6-Me$_2$C$_6$H$_3$)][PH$_2$CH=CHCH$_3$].

allowed. We trust that the present results may be helpful for designing new coordinatively unsaturated complexes as well as for elucidating the key steps in the metal promoted CH bond activation of saturated hydrocarbons.

Experimental Section

All reactions were carried out under an argon atmosphere using standard Schlenk techniques. The ruthenium complex **1** was prepared according to literature procedure.[5] All other chemicals were purchased from Aldrich and used without further purification. NMR measurements were recorded on a Bruker AC 200 spectrometer. Infrared measurements were obtained using a Nicolet Magna 550 series FT-IR spectrometer. Elemental analyses (C, H, N, I) were performed by the Microanalytical Laboratory of our department.

NMR Data for 1. ^{1}H NMR (200.1 MHz, CD$_2$Cl$_2$, −50 °C, TMS): δ = 7.45−6.75 (m, 26H; aromatic protons), 2.37 (d, J_{HP} = 5.1 Hz, 6H; CH_3), 1.30 (s, 6H; CH_3). ^{13}C{^{1}H} NMR (50.3 MHz, CD$_2$Cl$_2$, −50 °C, TMS): δ = 142.6 (s; CMe), 142.1 (*pseudo* t, J_{CP} = 8.8 Hz; CMe), 133.7 (*nonbinomial* qnt, *ipso*-C$_6$H$_3$), 132.8 (*pseudo* t, J_{CP} = 4.3 Hz; *o*-C$_6$H$_5$), 131.4 (*nonbinomial* qnt, *ipso*-C$_6$H$_5$), 131.0 (s; *p*-C$_6$H$_3$), 130.2 (s broad; *m*-C$_6$H$_5$), 129.7 (s; *p*-C$_6$H$_5$), 128.6 (*pseudo* t, J_{CP} = 5.3 Hz; *m*-C$_6$H$_3$), 127.9 (*pseudo* t, J_{CP} = 5.1 Hz; *m*-C$_6$H$_5$), 23.7 (s; CH_3), 10.1 (*pseudo* t, J_{CP} = 11.8 Hz; CH_3). ^{31}P{^{1}H} NMR (81.0 MHz, CD$_2$Cl$_2$, −50 °C, H$_3$PO$_4$): δ = 56.2.

Synthesis of 2. Complex **1** (300 mg, 0.400 mmol) and NaI (1.20 g, 8.00 mmol) were suspended in 8 mL of acetone, and the mixture was stirred overnight. The solvent was evaporated, and the product was extracted with CH$_2$Cl$_2$ and precipitated with methanol. The resulting brown product was filtered and dried under reduced pressure. Yield: 270 mg (72%). Anal. Calcd for C$_{40}$H$_{38}$I$_2$P$_2$Ru: C, 51.3; H, 4.1; I, 27.1. Found: C, 50.9; H, 4.0; I, 27.3. ^{1}H NMR (200.1 MHz, CDCl$_3$, 20 °C, TMS): δ = 7.45−6.85 (m, 26H, aromatic protons), 1.88 (d, J_{HP} = 4.7 Hz, 6H, CH_3), 1.30 (s, 6H, CH_3). ^{13}C{^{1}H} NMR (50.3 MHz, CDCl$_3$, 20 °C, TMS): δ = 142.7 (s, CMe), 142.6 (*pseudo* t, J_{CP} = 8.8 Hz, CMe), 135.5 (*nonbinomial* qnt, *ipso*-C$_6$H$_3$), 135.4 (*nonbinomial* qnt, *ipso*-C$_6$H$_5$), 133.6 (*pseudo* t, J_{CP} = 4.4 Hz, *o*-C$_6$H$_5$), 130.9 (s, *p*-C$_6$H$_3$), 130.4 (*pseudo* t, J_{CP} = 3.0 Hz, *m*-C$_6$H$_5$), 129.8 (s, *p*-C$_6$H$_5$), 128.8 (*pseudo* t, J_{CP} = 6.1 Hz, *m*-C$_6$H$_3$), 127.8 (*pseudo* t, J_{CP} = 5.1 Hz, *m*-C$_6$H$_5$), 24.0 (s, CH_3), 10.0 (*pseudo* t, J_{CP} = 12.2 Hz, CH_3). ^{31}P{^{1}H} NMR (81.0 MHz, CDCl$_3$, 20 °C, H$_3$PO$_4$): δ = 60.0.

Synthesis of 3. The synthesis of **3** was carried out as described for **2** by using NaOCN in place of NaI. Red product, yield: 209 mg (68%). Anal. Calcd for C$_{42}$H$_{38}$N$_2$O$_2$P$_2$Ru: C, 65.9; H, 5.0; N, 3.7. Found: C, 65.7; H, 5.0; N, 3.5. ^{1}H NMR (200.1 MHz, CDCl$_3$, 20 °C, TMS): δ =

7.52−6.82 (m, 26H, aromatic protons), 2.02 (s broad, 6H, CH_3), 1.42 (s broad, 6H, CH_3). ^{13}C{^{1}H} NMR (50.3 MHz, CDCl$_3$, 20 °C, TMS): δ = 142.0 (s broad, CMe), 133.7 (*nonbinomial* qnt, *ipso*-C$_6$H$_3$), 132.5 (*pseudo* t, J_{CP} = 4.7 Hz, *o*-C$_6$H$_5$), 131.4 (s, *p*-C$_6$H$_5$), 131.2 (*nonbinomial* qnt, *ipso*-C$_6$H$_3$), 130.1 (s, *p*-C$_6$H$_5$), 129.8 (s broad, *m*-C$_6$H$_3$), 128.6 (*pseudo* t, J_{CP} = 5.1 Hz, *m*-C$_6$H$_5$), 128.2 (s, NCO) 23.5 (s, CH_3), 9.4 (s, CH_3). ^{31}P{^{1}H} NMR (81.0 MHz, CDCl$_3$, 20 °C, H$_3$PO$_4$): δ = 60.3. IR (Nujol): 2239 cm^{-1} (NCO).

Kinetic Analysis. The ruthenium complex **1** (20 mg) was dissolved in 0.5 mL of CDCl$_3$, and the ^{1}H NMR spectra were recorded over the temperature range 262−327 K, using methanol to calibrate the probe temperature. In the slow exchange limit, two signals with the frequency difference $\Delta\nu$ were observed for the *o*-methyls. Simulations of the dynamic NMR spectra were carried out using the program DNMR5,[79a−c] which is available from the Quantum Chemical Program Exchange. The rates of exchange as a function of the temperature were determined by matching the experimental spectra with computed trial line shapes. Activation parameters ($\Delta H^{\ddagger}$, $\Delta S^{\ddagger}$, and $\Delta G^{\ddagger}$) were calculated from measured rate constants and temperatures using the Eyring equation k = $(k_B/h)T \exp(-\Delta H^{\ddagger}/RT) \exp(\Delta S^{\ddagger}/R)$, where k_B is Boltzmann's constant, h is Planck's constant, and R is the ideal gas constant.[36] Error analysis for $\Delta H^{\ddagger}$, $\Delta S^{\ddagger}$, and $\Delta G^{\ddagger}$ was based on Monte Carlo simulation with the SOLVERSTAT program[79d] and incorporated a ±1 K error in temperature and a ±2% error in the rate constant (±5 K and ±1 Hz in frequency difference for coalescence data).

Single-Crystal Neutron Diffraction Study on RuCl$_2$[PPh$_2$(2,6-Me$_2$C$_6$H$_3$)]$_2$ (1·Toluene). Single crystals, suitable for the neutron diffraction study, were grown in a temperature gradient from a solution of **1** in toluene. The selected sample, dark red in color, had dimensions 3.25 × 0.75 × 0.40 mm and had some surface powder. The crystal, which proved to be air- and moisture-stable, was fixed on a vanadium pin using a two component glue (Kwikfill). Then, it was mounted on the Eulerian cradle of the thermal neutron four-circle diffractometer D19 at the ILL, equipped with a 2-stage Displex cryorefrigerator[80] and a 64° × 4° position sensitive detector.[81] The crystal was cooled at 2 deg per minute to 100 K while two strong reflections were monitored. No change in crystal mosaicity was observed, and the reflection profiles

(79) (a) Stephenson, D. S.; Binsch, G. *J. Magn. Reson.* **1978**, *30*, 625. (b) Stephenson, D. S.; Binsch, G. *J. Magn. Reson.* **1978**, *32*, 145. (c) Stephenson, D. S.; Binsch, G. *QCPE* **1978**, *10*, 365. (d) Comuzzi, C.; Polese, P.; Melchior, A.; Portanova, R.; Tolazzi, M. *Talanta* **2003**, *59*, 67.
(80) Archer, J.; Lehmann, M. S. *J. Appl. Crystallogr.* **1986**, *19*, 456.
(81) Thomas, M.; Stansfield, R. F. D.; Berneron, M.; Filhol, A.; Greenwood, G.; Jacobe, J.; Feltin, D.; Mason, S. A. *Position-Sensitive Detection of Thermal Neutrons*; Convert, P., Forsyth, J. B., Eds.; Academic Press: London, U.K., 1983; p 344.

were acceptable at 100 K. Low-angle reflections were measured with a wavelength of 1.3072(1) Å, giving refined unit cell dimensions at 100 K from 178 strong reflections (ILL program Rafd19),[81] min and max 2-θ used 15.2° and 90.2°. The space group was confirmed as triclinic $P\bar{1}$ at 100 K. Slight twinning was observed, typical of larger crystals of this complex. The volume of the minor component was about 20% of that of the major component. Since the reflections from both components were successfully indexed, it was decided to continue data collection with the given crystal. In fact using a smaller untwinned crystal would produce counting statistics inadequate for a reasonable refinement, given the limited availability of beam time. To improve counting statistics, the wavelength was increased to 1.5364(1) Å and data collection continued in equatorial geometry but retaining any nonequatorial reflection observed coincidentally. Most of the unique higher angle reflections (up to a 2-θ value of 114°) were recorded (ILL programs Hklgen and Mad),[81] typically with 31 ω steps of 8.7 s (time). Three standard reflections were measured every 100 reflections, and showed no significant variation. Bragg intensities were integrated in 3-d using the ILL program Retreat,[82] and 2226 high angle data were used to get the final cell dimensions (Rafd19).[81] Observable reflections which were found to be significantly miscentered (13 at 1.3072 Å and 291 at 1.5364 Å) were rejected as probably contaminated by the minor twin component. The intensities were corrected for attenuation by the cylindrical V and Al heat shields (minimum and maximum transmission coefficients 0.8624 and 0.8981 at 1.3072 Å; 0.8349 and 0.8901 at 1.5364 Å), and by the crystal itself ($\mu_{neutron}$ = 0.221 mm^{-1} at 1.3072 Å and 0.239 mm^{-1} at 1.5364 Å, minimum and maximum transmission coefficients 0.8826 and 0.9181 at 1.3072 Å; 0.8595 and 0.9120 at 1.5364 Å) with the program D19abs, based on the ILL version of the CCSL system.[83] Overall, 428 usable reflections were recorded at 1.3072 Å and 5331 at 1.5364 Å yielding, after scaling and merging, 4058 unique reflections: R_{int} = 0.0369. The accuracy of the data set was improved by applying a twin correction,[84] i.e., by rejecting and separating some reflections that were significantly contaminated. Structure refinement was carried out using SHELXL-97 with the HKLF 5 option.[85] A total of 5468 reflections were used for full-matrix least-squares refinement where $\sum w(F_o{}^2 - F_c{}^2)^2$ was minimized by adopting a SHELXL-97 weighting scheme. After preliminary refinement, difference Fourier maps clearly revealed all of the hydrogen atom positions. All atoms of the asymmetric unit were refined anisotropically, giving a final R-value of 0.0641 [R1, $I_o > 2\sigma(I_o)$] and 0.1305 [wR2, all data], respectively (GOF = 1.123). The coherent scattering amplitudes used in the refinement were those tabulated by Sears.[86] The ruthenium complex shows no disorder, and the solvent toluene also appears well-ordered with full occupancy. Details of the neutron experiment, data reduction, and final structure refinement calculation are summarized in Table 4.

Computational Details. The model complexes reported herein were optimized with hybrid density functional theory (DFT) using Becke's three-parameter hybrid exchange-correlation functional[87] containing the nonlocal gradient correction of Lee, Yang, and Parr[88] (B3LYP) within the Gaussian98 program.[89] All optimized structures were confirmed as minima by calculation of numerical vibrational frequencies. A collection of Cartesian coordinates and total energies for all of the optimized molecules are available from the authors upon request. Basis sets for ruthenium utilized the effective core potentials of Hay and Wadt[90] with the associated double-ζ valence basis functions. The basis set used for the remaining atomic species was the 6-31G one with the important addition of the polarization functions (d, p) for all atoms, including the hydrogens.

Supporting Information Available: Tables of crystal and data collection parameters, atomic coordinates, bond lengths, bond angles, and thermal displacement parameters for **1** in .cif format. A justification of the outlier behavior of the complexes SAKWUW and QIVHEY in Figure 6. This material is available free of charge via the Internet at http://pubs.acs.org.

JA038986A

Table 4. Crystallographic Data for RuCl$_2$[PPh$_2$(2,6-Me$_2$C$_6$H$_3$)]$_2$ (**1**·Toluene)

chem formula	C$_{40}$H$_{38}$Cl$_2$P$_2$Ru, C$_7$H$_8$
fw	844.75
color/shape	purple/needle
cryst size [mm]	3.25 × 0.75 × 0.40
cryst syst	Triclinic
space group	$P\bar{1}$ (No. 2)
a [Å]	10.533(1)
b [Å]	12.728(1)
c [Å]	14.913(1)
α [deg]	89.465(6)
β [deg]	89.799(6)
γ [deg]	96.143(6)
V [Å^3]	1987.7(3)
Z	2
T [K]	100
radiation [Å]	neutron at 1.3072
radiation [Å]	neutron at 1.5364
ρ_{calcd} [g cm^{-3}]	1.411
μ (neutron at 1.3072 Å) [mm^{-1}]	0.221
μ (neutron at 1.5364 Å) [mm^{-1}]	0.239
F_{000}	872
Θ-range [deg]	2.95−56.88
data collcd [h,k,l]	h, −11/11; k, −13/13; l, −14/16
no. of rflns collcd at 1.3072 Å	428
no. of rflns collcd at 1.5364 Å	5331
no. of rflns for HKLF 5 refinements	5468
no. of obsd rflns [$I_o > 2\sigma(I_o)$]	4930
no. of indep rflns, R_{int}	4058, 0.0369
no. of params refined	884
R1, wR2, S [$I_o > 2\sigma(I_o)$]	0.0641, 0.1261, 1.123
R1, wR2, S [all data]	0.0727, 0.1305, 1.123
max and av shift/error	0.00, 0.00
max/min $\Delta\rho$ [fm Å^{-3}]	−0.70, 0.72

(82) Wilkinson, C.; Khamis, H. W.; Stansfield, R. F. D.; McIntyre, G. J. *J. Appl. Crystallogr.* **1988**, *21*, 471.
(83) Matthewman, J. C.; Thompson, P.; Brown, P. J. *J. Appl. Crystallogr.* **1982**, *15*, 167.
(84) Massa, W. *TWINXLI 1.1*; University of Marburg: Marburg, Germany, 1998.
(85) Sheldrick, G. M. *SHELXL-97*; University of Göttingen: Göttingen, Germany, 1998.
(86) Sears, V. F. *Neutron News* **1992**, *3*, 26.
(87) Becke, A. D. *J. Chem. Phys.* **1993**, *98*, 5648.
(88) Lee, C.; Yang, W.; Parr, R. G. *Phys. Rev. B* **1988**, *37*, 785.
(89) Frisch, M. J.; Trucks, G. W.; Schlegel, H. B.; Scuseria, G. E. M.; Robb, A.; Cheeseman, J. R.; Zakrzewski, V. G.; Montgomery, J. A.; Stratmann, R. E.; Burant, J. C.; Dapprich, S.; Millam, J. M.; Daniels, A. D.; Kudin, K. N.; Strain, M. C.; Farkas, O.; Tomasi, J.; Barone, V.; Cossi, M.; Cammi, R.; Mennucci, B.; Pomelli, C.; Adamo, C.; Clifford, S.; Ochterski, J.; Petersson, G. A.; Ayala, P. Y.; Cui, Q.; Morokuma, K.; Malick, D. K.; Rabuck, A. D.; Raghavachari, K.; Foresman, J. B.; Cioslowski, J.; Ortiz, J. V.; Stefanov, B. B.; Liu, G.; Liashenko, A.; Piskorz, P.; Komaromi, I.; Gomperts, R.; Martin, R. L.; Fox, D. J.; Keith, T.; Al-Laham, M. A.; Peng, C. Y.; Nanayakkara, A.; Gonzalez, C.; Challacombe, M.; Gill, P. M. W.; Johnson, B. G.; Chen, W.; Wong, M. W.; Andres, J. L.; Head-Gordon, M.; Replogle, E. S.; Pople, J. A. *Gaussian 98*, revision A.7; Gaussian, Inc.: Pittsburgh, PA, 1998.
(90) Hay, P. J.; Wadt, W. R. *J. Chem. Phys.* **1985**, *82*, 299.